SOLAR ULTRAVIOLET RADIATION AND THE ROLE OF RECA IN MARINE BACTERIA

By

MELISSA G. BOOTH

Bachelor of Science

Oklahoma State University

Stillwater, OK

1991

Submitted to the Faculty of the
Graduate College of the
Oklahoma State University
in partial fulfillment of
the requirements for
the Degree of
DOCTOR OF PHILOSOPHY
December, 1997

SOLAR ULTRAVIOLET RADIATION AND

THE ROLE OF RECA IN

MARINE BACTERIA

Thesis Approved:

Robert V. Miller

Thesis Advisor

Dean of the Graduate College

ACKNOWLEDGMENTS

I wish to extend my sincere gratitude to my graduate committee members, Dr. Steve Schafer, Dr. Wade Jeffery, Dr. Robert Burnap, Dr. Kim Burnham and Dr. Robert Miller for their time and assistance. Dr. Robert Miller has been more than an advisor, and his special encouragement, patience and support will always be remembered. I would also like to thank Dr. Curtis Suttle, Dr. Steven Wilhelm and Dr. Rick Coffin for their assistance with research cruises and support. April Rowe, Shelley Wedel and Ryan Schafer, undergraduate assistants, deserve recognition for their willingness to learn by doing.

I thank my parents, Wayne and Sharon Booth, for their continued support and encouragment, and for providing refuge in times of need. My dear friend, Roxy Johnston, has been a never-ending sympathetic ear. LeAnna Hutchinson, Trent Taylor, and Margaret "Pope" Brumsted have done wonders for my self-esteem. To list all the coworkers and friends that have helped and cheered me at OSU and various research cruises would be impossible. To them, I am forever grateful. I wish to express my love to my family, friends and Dr. Miller. I could never have completed this endeavor without you.

TABLE OF CONTENTS

LIST OF TABLES

LIST OF FIGURES

CHAPTER I

INTRODUCTION

It has been clearly established that solar ultraviolet radiation (UV-R) is increasing as a result of ozone depletion. This has been demonstrated by both direct measurements and studies of various biological systems (16, 25, 53, 70, 72). However, until recently very little information was published on the fate of bacterioplankton following exposure to UV-R in the marine environment. At the base of most oceanic food webs, bacterioplankton are believed to process 14-76% of primary production depending on season and regional variation (3), as well as functioning as mineralizers and secondary producers consumed by higher trophic levels. An upset in bacterial community structures may have dramatic effects such as disruption of food webs, changes in dominant phytoplankton species, altered elemental cycles and biological interactions (13, 22, 25, 28).

Research indicates that UV-R imposes chronic stress on marine bacteria (4). Bacteria are small and their genetic materials comprise a significant portion of their cellular volume. Therefore, bacterial genetic material is highly susceptible to solar UV-R (34). When bacterial deoxyribonucleic acid (DNA) is damaged, the cells respond by inducing several mechanisms to repair injured sites. *recA* is a key player in this response,

functioning as a regulator of DNA-damage repair (43). Previously, the response of the *recA* gene to solar UV-R induced damage was unknown. However, Kidambi et al. showed that *recA* is induced by solar UV in the soil and freshwater microorganism, *Pseudomonas aeruginosa* (39).

The purpose of this study was to determine whether specific wavelength ranges within the solar UV spectrum induce *recA*, and if this induction could be detected *in situ* among marine microorganisms. Additionally, the relationship of *recA* induction, cell survival and the accumulation of DNA damage within UV-R-exposed populations was investigated to develop a standard to which future studies can be compared.

This research is part of a larger study investigating the impact of UV-R on marine bacteria. Several of the results obtained here are being observed for the first time and are valuable in themselves for the specific questions they address. Findings on bacterial survival, production and recovery cannot however, be extrapolated to higher trophic levels in the dynamic marine environment. Yet, by developing techniques, dosimeters, and standards that can be readily applied, the potential scope of future studies becomes broader. Utilizing the information and tools developed by this work, other scientists can investigate multiple aspects of particular questions simultaneously which will lead to more accurate predictions to the real question, "How will continued ozone depletion and UV-R increases affect global ecosystems?"

CHAPTER II

LITERATURE REVIEW

Ozone depletion. The ozone layer (altitude 15-30 Km) is the earth's shield in the stratosphere (altitude 10-50 Km), protecting the surface below from solar ultraviolet radiation (UV-R) (71). Ozone is composed of three oxygen molecules and is measured in Dobson units (DU) to quantify the total amount of ozone occupying a column overhead. Ozone exists in a photochemical equilibrium. Ultraviolet radiation splits oxygen (O_2) into two reactive oxygen (O) atoms which then combine with intact oxygen molecules (O_2) to form ozone (O_3). Under the appropriate conditions, chloride (Cl^-) can act as a catalyst by splitting O_3 into one O atom and one O_2. The free O will quickly pair with another to form an intact O_2. Thus, the net result of Cl- catalysis is a loss of O_3. Ultraviolet radiation and temperatures in the -80°C range are necessary for this reaction to occur (71, 72, 73). This process is a chain reaction in which each Cl^- remains unchanged and can destroy up to 100000 O_3 molecules (73). Chlorofluorocarbons, once heralded for their stability, non-flammability, low toxicity and low cost, have been extensively used as coolants and

propellants, and are now believed to be greatly responsible for ozone depletion (63). Other chlorine-containing compounds such as methyl chloroform, a solvent, carbon tetrachloride, an industrial chemical; halons, used in fire extinguishers; and methyl bromide, a produce and soil fumigant, also release chloride or bromide into the stratosphere which destroys ozone.

Under natural conditions, ozone concentrations vary predictably with sunspots, seasons, and latitude. Depletions were first observed by ground-based measurements from Halley Bay on the Antarctic coast between 1980 to 1984 (14). In 1985 the British Antarctic Survey published findings of a depletion in springtime ozone (73). Since then the worldwide scientific community has agreed that ozone depletion is occurring in the stratosphere largely due to the release of man-made chemicals (83). In Antarctica, ozone levels fall 60% during "hole" events in the worst years. An already low concentration of 300 DU in austral spring can drop below 150 DU (89).

Why Antarctica? As the stratosphere warms, the Antarctic air is isolated forming a polar vortex in which polar stratospheric clouds and reactive stratospheric clouds sediment and denitrify reservoir compounds, $CLONO_2$ and HCl. Photolysis occurs in the upper and lower atmosphere in springtime, releasing chlorine which has built up over the winter, which in turn rapidly destroys ozone. At this time the temperature within he polar vortex is -80°C, but the "hole" disappears when temperatures rise

above -80°C. Ozone depletion results in decreased absorption of UV-B by the stratosphere and increased UV-B penetration to the earth's surface (14, 16). This phenomenon is measured in RAFs (Radiation Amplification Factors) which is the percent increase in UV-R for each 1% reduction in the ozone column (83). At present, rough estimations indicate a 2-3% increase in UV-B for each 1% decrease in total ozone (81). Zerefos et al. (89) have measured a 1.9% per year decline in ozone over Antarctica from 1990 to 1995 resulting in a 4% per year increase in UV-R at 305 nm. Specifically, there is an increase in shorter wavelengths, or the more bioactive portion of the UV spectrum, without a proportional increase in longer wavelengths involved in photosynthesis and photorepair processes (70).

Ultraviolet radiation. UV-R is electromagnetic radiation at wavelengths shorter than the visible region and longer than the x-ray region: 10-400 nm (Fig. 1) (29). Solar UV-R consists of far UV-R (100-200 nm), middle UV-R (200-300 nm), and near UV-R (300-400 nm). Previous studies of microorganisms' response to solar UV-R have placed these wavelengths in different categories: UV-A (320-400 nm), UV-B (280-320 nm), and UV-C (100-280 nm). To study responses to environmentally relevant UV-R, one must consider which wavelengths are being absorbed by O_3 and will be affected by a decrease in O_3. Wavelengths below 200 nm (a component of UV-C) are completely absorbed by O_2 in the atmosphere. A portion of radiation is absorbed by O_2 (70). Ozone shows a strong absorption band starting at 255 nm and extending beyond 360 nm. The absorption

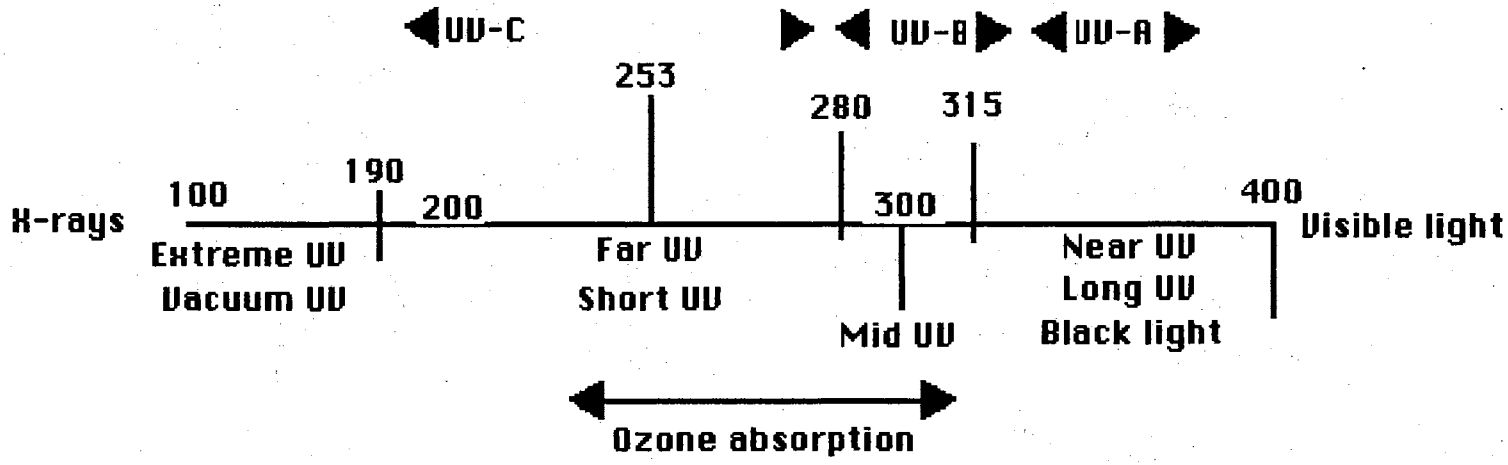

Fig. 1 The major components of the UVR spectrum

coefficient falls off rapidly with wavelength, and reduction of solar flux is a function of increasing wavelength. Therefore, studies of increased UV-R due to ozone depletion should focus on the wavelengths in the UV-B and UV-A ranges.

In the marine environment, UV-R has already been implicated in coral bleaching, decreased phytoplankton production, decreased photosynthesis and reduced bacterial activity (1, 22). Penetration of UV-B is the greatest cause of concern for humans, plants, animals and marine life when discussing a thinning ozone layer (13). These wavelengths are responsible for most damage to organisms by sunlight. UV-B damages fish eggs and krill, reduces recruitment and adversely affects trophic transfer of productivity due to solar UV-B induced damage (41). Karentz et al. (37) showed biologically harmful wavelengths of UV-B penetrating to a depth of 10 meters in the Antarctic ocean in October when the ozone "hole" occurs. In November, when ozone levels recovered, no biological wavelengths of UV-B were detected at 10 meters. This clearly indicates that levels of UV-B radiation will increase with a decrease in stratospheric ozone (37).

In sunlight reaching the earth's surface UV-A is present in the highest intensity (7), and has been shown to impact cell viability at higher rates than UV-B (24). UV-A wavelengths are thought to be responsible for 50% of the total inhibition of photosynthesis by UV-R (21, 24, 25). Both UV-A and UV-B were found to suppress photosynthetic rates in *Laminaria digittata* (brown algae) (15). Additionally Herrmann et al. (23) demonstrated decreased growth, degradation of pigments, decreased motility, loss of

orientation, and reduced photosynthesis among phytoplankton after UV-R stress. Detrimental affects of increasing UV-R will most likely result in a weakened food web and shifts in species composition (13).

Bacteria in the Marine Environment. The marine environment contains a plethora of different bacterial species, but a large percentage are still considered unculturable (59). Though a majority live in the anaerobic sediment zone, bacterioplankton comprise 10-50% of the phytoplankton biomass in the euphotic zone (21) and reside in the center of the microbial food web. Carbon recycling via the "microbial loop" evolved over the past one-million years, and we are just now beginning to understand the relationship of DOM (dissolved organic matter), heterotrophic bacteria, flagellates and phytoplankton. The microbial food web is the major retainer of organic carbon in aquatic ecosystems, and influences of UV-R on the various participants within the loop are of great concern to understanding how overall productivity may ultimately be impacted by depletion of stratospheric ozone.

Because of their small size (35), bacteria are highly susceptible to UV-R. These nano- and pico-plankton (0.1-10 μm) convert 80% of phytoplankton primary production to dissolved particulate organic matter (18) . Bacterioplankton enzymatically cleave DOM. Herndle (22) showed that solar UV-R suppresses bacterial production and proliferation, while at the same time photochemically destroying bacterial enzymes. Photooxidation of DOM increases its availability and can stimulate bacterial growth. However, Herndle speculated that increased levels of

labile DOM in the surface layers of the ocean as a result of increasing UV-B will lead to alterations of dominant species (22). Results of studies have indicated that photodegradation of DOM does lead to increased UV-B penetration. This leads to enhanced formation of dissolved inorganic carbon and carbon monoxide, alterations within sulfur cycles, and decreased bioavailability of trace nutrients (88).

On the other hand, Kaiser and Herndle recently showed that DOM photolytically cleaved in the surface layers and subsequently mixed along with bacterioplankton into deeper layers is taken up rapidly, leading to enhanced bacterial activity (36). They hypothesize that as highly-damaged bacteria from the surface layer are mixed into deeper layers where harmful wavelengths are attenuated and longer wavelengths can activate repair mechanisms, photolyzed DOM is readily taken up and metabolized by recovering microorganisms.

Research indicates that UV-R imposes chronic stress on marine bacteria. In the Chesapeake Bay, microcosm studies were conducted to examine the uptake of amino acids using microautoradiography. Uptake increased when bacteria were shaded from UV-R, and decreased in exposed areas (4). Sunlight has been shown to inactivate ammonia oxidation in *Nitrosomonas* sp. and inhibit nitrification in sea-surface films (25, 26). Aquatic cyanobacteria assimilate 35-million tons of nitrogen each year. UV-R (UV-B) inhibits nitrogenase. Bacterioplankton mediate geochemical cycling of sulfur, phosphorus, and nitrogen in addition to their roles in secondary and primary production. Changes in this commu-

nity due to altered exposure to UV-R could have extensive effects on the entire ecosystem (1, 13, 34, 35).

DNA damage. UV-C (100-280 nm) is the most energetic wavetype causing direct DNA damage in the form of cyclobutane pyrimidine dimers (CPDs). A cyclobutane dimer is a four-membered ring structure between adjacent pyrimidines (thymine or cytosine) resulting from the saturation of their 5 and 6 carbon double bonds. These lesions block DNA replication by inhibiting the action of DNA polymerases and lead to gene inactivation. UV-C also causes DNA-protein crosslinks which are amino acids covalently linked to pyrimidines of DNA as well as DNA-DNA strand-to-strand crosslinks. Most studies of UV-R effects on molecular responses in microorganisms have been done using wavelengths in the UV-C range. UV-B (280-320 nm) also results in direct DNA damages such as CPDs. However, dimers more often involve cytosine at these higher wavelengths. Other photoproducts such as pyrimidine (6-4) pyrimidone (6,4PD) and its valence photoisomer, Dewar pyrimidone, are produced at significantly increased levels (9, 20, 46, 48). Specifically these photoproducts are produced at 313 nm at a dose between 100-500 J/m^2. UV-B also induces photohydrates (33). (6-4) pyrimidines are linkages between the 6 carbon of a 3' cytosine or thymine and the 4 carbon of a 5' cytosine. These products are thought to be more mutagenic than dimers (61). Between 254-302 nm the action spectrum, or wavelength-dependent response, of DNA damage remains the same. However, the range from 310 nm to 320 nm induces a higher ratio of 6,4PDs (33).

There are several mechanisms of UV-A (320-400 nm) action which are poorly understood and complex. UV-A produces lesions in which DNA remains the critical target but is not the primary chromophore (56,57,64). UV-A is poorly absorbed by protein and nucleic acid, but is easily absorbed by other cellular chromophores. Many studies speculate that an intermediate molecule, such as heme, flavin, or bilirubin absorbs the incident UV-A photon and transfers the energy to DNA (7). Other studies have shown that thiolated tRNA molecules are inactivated by UV-A (32, 55). UV-A produces a crosslink of the 4-thiouracil with cytosine, thus inactivating the acetylation capacity of these tRNAs. This inactivation leads to abrupt cellular growth delay and reduction of cell size.

Hydrogen peroxide and other reactive oxygen species generated by UV-A cause significant DNA damage. Hydrogen peroxide-induced damage is attributed to a Fenton reaction that generates OH· from H_2O_2, DNA-bound iron, and a source of reducing equivalents (30). Hydrogen peroxide also reacts with O_2^- to yield OH· which damages DNA. Klamen and Tuveson (40) showed that UV-A-generated singlet oxygen ($^1O_2$) reacts with unsaturated fatty-acid components of membrane phospholipids leading to generalized membrane damage and resultant lethality. Peak and Peak (57) found that O_2 is required for 90% of lethal events in *Escherichia coli* exposed to UV-A.

DNA appears to be the principal target for UV-A killing of cells in most circumstances with single-stranded breaks being the most probable lesion (32). This is supported by the following evidence including the above

mechanisms. First, oxygen enhances lethality and breakage whereas DABCO and glycerol inhibit these effects. Second, *E. coli* strains with different UV-A sensitivities, also differ in their accumulation rate of DNA SSB's. Third, strains lacking ^{4}Srd (thiolated tRNA) are less susceptible to UV-A lethality and DNA breakage.

Other mechanisms may include agents involved in DNA integrity such as ribonucleoside diphosphate reductase. Peters (58) demonstrated that UV-A exposure resulted in inactivation of ribonucleotide reductase *in vivo*. Sensitivity to the effects of UV-A depends greatly on the growth phase of a bacterial culture (32). Actively growing cells are often much more sensitive to inactivation than are stationary phase cells.

Several endogenous compounds act as the primary chromophore or photosensitizer in bacterial cells. Most often their activity is dependent on the presence of oxygen. Other endogenous photosensitizers include chlorophyll, heme, and protoporphyrin. Cyclobutane dimers are formed more effectively in the presence of organic substances which act as exogenous photosensitizers (74). Flavins, thiazines, acridines, xanthenes, porphyrins, and psoralens are other examples of exogenous photosensitizers. Several environmental pollutants and domestic chemicals are believed to have significant DNA-photosensitizing activity (PSA) (11). Marine microorganisms, especially those living in coastal areas, are likely bombarded with several of these pollutants daily. Photosensitizers should be considered when examining the impact of increasing UV-R in the marine environment.

DNA repair. The response of organisms to ultraviolet radiation is highly dependent on the spectral composition of the source, the intensity (dose-rate), and the exposure duration. Cellular defenses against UV-R vary among organisms. Many marine organisms produce chemical compounds or pigments to absorb UV-R energy and provide direct protection from UV-R (38, 42, 66). In addition, organisms may use several different mechanisms of DNA repair to reverse damage from UV-R. Several secondary mechanisms of photoreversal and DNA repair that are recognized but are as yet uncharacterized and poorly understood are beyond the scope of this study and will not be addressed (17). There are four major mechanisms by which cells repair DNA: (1) photoenzymatic repair or photoreactivation (2) recombinational repair (3) nucleotide-excision repair, and (4) SOS-mutagenic repair. Photoreactivation, first observed forty years ago in *Streptomyces griseus*, utilizes the enzyme photolyase and visible light to reverse cyclobutane dimerization and other DNA photoproducts (52). DNA photolyases are flavin-containing enzymes which specifically bind photoproducts in DNA and perform light-dependent (300-450 nm) reversion. These enzymes are universal in animals, algae, bacteria and other organisms (87). In the marine environment, photoreactivation is essential for maintenance of high concentrations of viruses in surface waters and likely plays a direct or indirect role in regulating bacterial population density as well (85).

Recombinational repair is a complex process in which damaged DNA is reconstructed through DNA replication and strand exchange facilitated by the *recA* gene. Post-replication recombinational exchange

which repairs daughter-strand gaps or double-strand breaks occurs as well as pre-replication recombinational repair of gaps resulting from excised lesions within the DNA (43). These processes are *recA*-dependent. Excision repair is a more complex system which excises damaged bases, resynthesizes DNA in the damaged area, and ligates nicked strands. The*uvrABC* nuclease recognizes a dimer-induced distortion of the helix and produces a break on either side of the lesion. UV-R D (helicase II) releases the complex through protein-protein interaction. DNA polymerase I fills the gap (approx. 12 nucleotides) using the opposite strand as a template. DNA ligase repairs the gap (17). Bacteria regulate nucleotide-excision repair of UV-R damage to nucleic acids through the induction of a series of approximately 20 genes including *uvrABC* termed the SOS network. Central to the functioning of this network is the *recA* gene. The fourth major repair mechanism, SOS mutagenic DNA repair, is also encoded by this *recA*-regulated regulon. The *umuDC* operon controls mutagenic DNA repair. It appears to function by altering DNA polymerase III's proofreading fidelity.

The *recA*. gene. In addition to its synaptase function in recombination and its coprotease regulatory role in DNA repair processes, RecA, the protein product of the *recA* gene, is closely associated with mutagenesis. In *Escherichia coli*, RecA is required for recombination of chromosomal DNA via any of the known biochemical pathways. This protein functions as a synaptase requiring ATP hydrolysis and regions of ssDNA (single-stranded DNA) to carry out a variety of reactions in which ssDNA is

annealed to homologous ssDNA or to dsDNA (double-stranded DNA). Additionally, RecA regulates the induction of several repair genes in the SOS network (44). The SOS network is comprised of several operons which function in various cellular processes, although the majority appear to respond to stressful situations (17). The term 'SOS' is often misinterpreted as a last ditch effort by the cell to save itself. However, the original author coined the term to simply refer to this group of operons as a universal distress call (17). In response to an unidentified signal, RecA is activated and facilitates the cleavage of the SOS repressor, LexA. In non-stress situations LexA binds the SOS promoters suppressing transcription of the SOS genes including *recA* (43, 45, 82). The elusive activating signal of RecA is thought to be altered DNA replication. However, if stop-and-go DNA replication is the signal for the induction of RecA, one might ask why RecA is not activated by other ssDNA regions typically found in the lagging strand during the replication process? Most likely, the answer is simply kinetic. RecA either cannot polymerize on a single-stranded DNA region or remove single-stranded binding (ssb) protein before the replication complex has formed (17). But we can be certain that activated RecA is the cells' indicator of DNA damage.

RecA controls mutagenesis in two ways: (1) mediation of LexA cleavage allowing transcriptional derepression of the *umuDC* operon responsible for SOS mutagenesis, and (2) post-translational activation of the UmuD protein by coproteolytic cleavage similar to LexA cleavage. *umuDC* operon is solely responsible for SOS-associated mutagenesis. Increases up to 200-fold in mutability have been observed in 16 enterobacte-

ria following SOS-induction. Some species are completely non-mutable while others gain the response upon expression of an intact *umuDC* homolog. Elucidation of this response is difficult as the SOS network can be completely 'ON', completely 'OFF,' or partially induced. With RecA localized at the lesion, mutagenesis is believed to be the result of translesion replication. Interestingly, (6-4) photoproducts result in enhanced mutagenesis. These photoproducts give rise to larger distortions within the DNA helix, and RecA binds more efficiently to these lesions than cyclobutane dimers (61).

The activities of RecA described above were discovered using UV-C as the DNA-damaging agent. However, this protein also plays a role in response to solar UV-R. Tuveson found that *uvrA-recA* double mutants are highly sensitive to solar UV-R (78). Karentz and Lutze (37) used a *phr-1* (photoreactivation) *uvrABC* (excision repair) mutant for studies in Antarctica. However, an additional Rec- mutation made the cells susceptible to as little as 1-2 photoproducts per genome and cells died after 30 seconds of exposure to sunlight. Previous studies done by Miller and coworkers (39) indicate that *recA* plays a direct role in the bacterial response to UV-A and UV-B irradiation. They have found that *recA* mutants of *Pseudomonas aeruginosa,* a freshwater and soil inhabitant, are significantly more sensitive to UV-A and UV-B than are wild-type cells. When a functional *recA* gene was introduced into these RecA$^-$ mutant's, UV-A and UV-B resistance was restored significantly (39).

The *recA* gene is likely universally present in bacteria. It is a highly conserved genetic element found among prokaryotes (bacteria and

cyanobacteria) (43). The high level of structural and functional conservation of *recA* among highly divergent bacteria suggests that this gene originated very early in the evolution of prokaryotes (43). Organisms as distant as *E. coli* and *Synechococcus* species share 57% amino acid sequence identity. Other related enteric species share up to 100% sequence identity. Nucleotide sequences show similar sequence homology. Using Western analysis, RecA proteins from almost all tested species of prokaryotes cross-react with *E. coli* anti-RecA antisera (44). The regions responsible for ATP hydrolysis and binding, and interacting with ssDNA are highly conserved while other regions of the protein deviate (43). The carboxy-terminal implicated in coprotease activation lacks conservation which may suggest that SOS repressor-RecA interaction is species-specific. This would support observations of differing levels of SOS induction among various prokaryotic species (43). RAD1 appears to be the eukaryotic equivalent of *recA* (43). Because *recA* is widespread and has been found to function in a solar-UV-R response, it may be a good biological dosimeter for detecting bacterial response to UV-R-induced DNA damage.

Biological dosimeters and Action spectra. Biological and molecular dosimeters provide a simple tool to estimate the magnitude of a biological effect expected from a source of radiation. They may be used to substitute physical (radiometric) or chemical (actinometric) dosimeters for a given UV source requiring only a reproducible dose-response that can be calibrated against an accurate standard (79). Biological dosimeters cans also be used to provide a quantitative estimate of the magnitude of a given

biological effect to be expected from a variable polychromatic source such as sunlight (79). The major requirement for this case is that the spectral sensitivity of the dosimeter should correspond reasonably to the action spectrum of the biological end point of interest (79). Such dosimeters may fill a need for an accurate inexpensive method for monitoring biologically effective UV-R and predicting responses to increasing solar flux. Simple test systems have been used as biological dosimeters such as the uracil molecule, DNA, bacteriophages and bacteria (34, 35, 37, 60, 79, 83). Their action spectra agree quite well with that of DNA damage (9, 12, 68). Action spectra are defined as the measurement of a biological effect as a function of wavelength. The important issue in biological dosimetry of broad spectrum sources is related to how well the spectral dependence of the biological detection system matches the action spectrum for the biological effect of interest (37). Ideally, the spectral response of the dosimeter will be identical to that of the action spectra. In addition, dose-response kinetics and quantum yield should be the same throughout the wavelength region studied. Cellular and molecular shielding and scatter should be negligible at all wavelengths, or if not, should not vary. If this occurs, a constant Morowitz correction should be applied (64). The spectrum should be the same *in vivo* as *in vitro*. Finally, reciprocity of time and dose rate should be followed at all wavelengths. However, these ideal conditions are never met, and each action spectrum is of necessity a series of compromises (64).

The action spectra for several critical biological processes have been combined with physical radiation intensity data from spectroradiometer measurements (W/m^2) to determine the potential biological effectiveness of

the radiation on a particular biological system (9, 27). Effectiveness is essentially combining the action spectra for a given biological response and integrating it with spectral data for a given amount of ozone (27). Biological dosimeters have several advantages over weighted spectroradiometry. The greatest advantage being the ability to place such dosimeters anywhere anytime. Weather conditions greatly affect the intensity of incident UV-R, and the instantaneous data points of spectral analysis must be carefully corrected. Oppositely, a biological dosimeter automatically weights the incident UV-R components of sunlight in relation to the biological effectiveness of the different wavelengths and the interactions between them. A biological dosimeter registers total exposure, regardless of changes in weather, providing an accurate record of UV-R dose over a designated period, and a higher degree of accuracy than is possible to obtain from a conventional radiometric data set.

Karentz et al. (37) used a DNA-repair-deficient strain of *E. coli* to monitor UV radiation. Quantification of survival after exposure to solar UV-R at selected depths within the water column of the Antarctic ocean was used as a dosimetric measurement. Using filters provided the ability to distinguish lethality caused by specific wavelengths. Regan et al. (60) used naked DNA molecules as a solar UV-B dosimeter to avoid whole organism complications, such as shielding by chlorophyll or other pigmentation, variations in sensitivity and repair, or variations in movement of organisms. Using DNA established a "total dose" or maximum amount of damage that could be induced in DNA by UV-B. This method is useful for measuring amounts of ultraviolet radiation, but is not an accurate

measure of bacterial response. Jeffrey et al. (34, 35) also utilized DNA dosimeters to compare accumulation of CPDs in the dosimeters with CPD accumulation in natural bacterial assemblages. Exponential reduction in CPD formation was observed with depth in the water column in the DNA dosimeters and the bacterial community (34, 35). However, significant differences were observed. At the surface, CPD accumulation was about 50% less in the bacterial community compared to the purified DNA dosimeters. Below 3 m depth in the water column, much greater damage was observed in the bacterioplankton compared with the DNA dosimeters (34, 35). The results of these studies demonstrate the usefulness of DNA dosimeters, but also show their limitation in comparison to other dynamic biological systems such as the marine bacterioplankton community.

Presently, most action-spectra data have employed monochromatic wavelengths in the ultraviolet spectrum. Yet, various interactions (synergetic, additive or antagonistic) are possible between each wavelength region and must also be taken into account when studying a broad spectrum source (i.e. sunlight). To demonstrate the potential involvement of interactive effects resulting from solar radiation, studies implementing polychromatic radiation could be as valuable as traditional action spectra.

Accurate information is needed to assess the potential effects of increases in the UV radiation reaching the earth's surface due to the depletion of stratospheric ozone on a living organism. Of immediate use would be a series of action spectra for general biological effects that would typify responses to increased UV-R. The full UV-R range, applied in both monochromatic and polychromatic forms, would be preferable to estimate

all cellular responses including repair. Additionally, gathering information on repair rates in natural communities and comparing this with estimates of DNA damage may provide helpful insight on how marine bacterioplankton cope with increasing UV-R.

CHAPTER III

METHODOLOGY

This study addresses *recA* expression in *Vibrio natriegens* and natural marine bacterioplankton communities in response to ultraviolet radiation. Experiments were conducted in the laboratory under controlled conditions, and in the environment to elucidate *in situ* responses. Part of the task set forth was to test and develop methods for analyzing environmental samples for which procedures are outlined in full detail below.

***recA* in *Vibrio natriegens*.** *V. natriegans* (ATCC 14048) was chosen because it is ubiquitous in both coastal and open-ocean seawater making it a good representative of marine bacterioplankton. This organism is also easy to work with and easily obtainable. Southern blot analysis was done to demonstrate the existence of a *recA* gene within the *V. natriegens* genome. Chromosomal DNA from *V. natriegens* was isolated by the method of Saunders (65). Genomic DNA was digested at 37°C overnight with *Bgl* II as recommended by the manufacturer (New England Biolabs, Beverly, MA). *Vibrio anguillarium recA* was obtained from Dr. Marcelo E. Tomalsky to use as a probe (76). pMETSK$^+$, pBluescript®SK$^+$ (Stratagene, La Jolla, CA) containing the *V. anguillarium recA* on a 2.3 Kbp fragment was extracted from *E. coli* with a Wizard™ MiniPrep plasmid DNA

purification kit as recommended by the manufacturer (Promega, Madison, WI). The phagemid was digested 1 hour by manufacturer recommendations with *Hind* III (New England Biolabs) to produce the 2.3 Kbp fragment with the *V. anguillarium recA* and the 2.964 pBluescript®SK$^+$ fragment. The 2.3 Kbp band was extracted from a 0.8% agarose gel with the Gene Clean II®kit as recommended by the manufacturer (Research Products Intl. Corp., Mount Prospect, Il). *Bgl* II-digested *V. natriegens* genomic DNA was run overnight at 25 volts on a 1% agarose gel to achieve optimum separation. Bacteriophage Lamda DNA was included as a negative control and pMETSK$^+$ digested with *Hind* III as a positive control. An overabundance of 1 Kb DNA ladder (New England Biolabs) was also included to facilitate molecular weight estimation. DNA was transferred onto a Nytran®Plus nylon membrane (Schleicher & Schuell, Keene, NH) by vacuum blotting one hour. The membrane was pre-hybridized, hybridized using the 2.3 *recA* fragment from pMETSK$^+$ as a probe, and detected by a chemiluminescent substrate by the conditions described by the DIG/Genius™ system (Boehringer Mannheim Corp., Indianapolis, IN). Autoradiography demonstrated hybridization of the *V. anguillarium recA* fragment to a region approximately 7 Kbp within the *V. natriegens* genomic DNA (Fig. 2). Likewise, a positive signal was achieved when using the *E. coli recA* as a probe.

Cross-reactivity of purified *E. coli* RecA with *V. natriegens* RecA was tested by western analysis. 10 mls of a *V. natriegens* culture in logarithmic growth phase (60 to 80 Klett units [KU]) was centrifuged 5

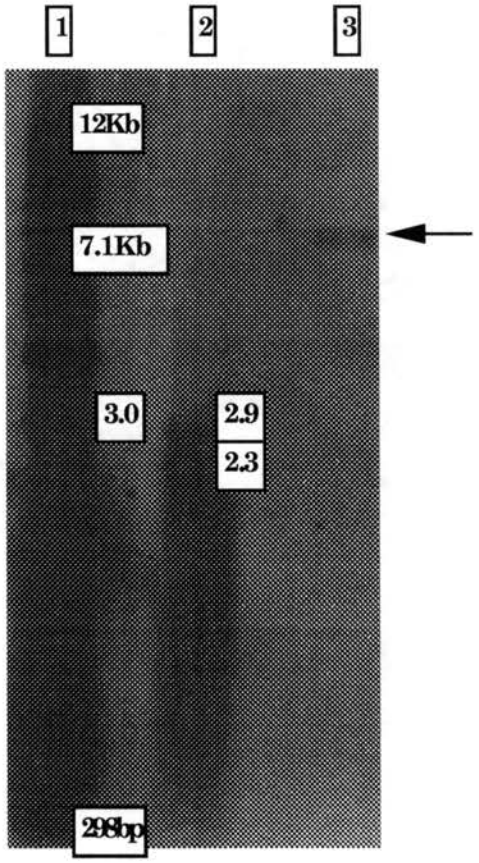

Figure 2. Autoradiograph of Southern blot demonstrating cross-hybridization of *V. anguillarium recA* with *V. natriegens*. Lane 1 is a 1 KB DNA ladder. Lane 2 is HindIII-digested pMETSK (pBluescriptSK+ with a 2.3 Kb HindIII fragment carrying the *V. anguillarium recA*). Lane three is BglII-digested *V. natriegens* genomic DNA.

minutes, 6000 rpm at room temperature, resuspended in 300 μl Protein Extraction Buffer (PEB) (50mM Tris-HCL, 2% SDS, 10% glycerol pH 6.8), and placed in a boiling water bath 5 to 10 minutes. Protein concentrations were determined using the Bio-Rad DC (detergent-compatible) protein assay kit (BioRad Laboratories, Hercules, CA). Three micrograms of total protein was separated on a 12% SDS-PAGE (polyacrylamide) gel at 100 volts for 1.5 hours. *E.coli* total protein was included as a positive control. The proteins were transferred to Immobilon™-P PVDF membrane (Millipore, Bedford, MA) by electroblotting using a Mini Trans-Blot Cell as recommended by the manufacturer (BioRad). Western analysis was done utilizing the BioRad Immune-Lite™ kit (BioRad). The primary antibody, a polyclonal preparation of *E. coli* anti-RecA, was used at a ratio of 1:5000 and incubated four hours. Chemiluminescent development and subsequent autoradiography demonstrated a strong cross-reactivity between the *E. coli* RecA and a region in the *V. natriegens* total protein extract corresponding to the expected approximate 40 KD molecular weight (44) (Fig. 3). *E. coli* anti-RecA was generously supplied by Dr. S. Kowalscykowski (University of California, Davis, CA) initially. Later, preparations were obtained from the OSU Hybridoma Center (Stillwater, OK).

RecA protein analysis. For all experiments conducted, immunological assessment of the concentration of RecA protein in total protein extracts was in general conducted as described by Miller and Kokjohn (25). Bacterial total proteins were extracted from either frozen polycarbonate filters or frozen cell pellets in PEB and placed in boiling water 5 to 10 minutes. Lowry protein assays were performed to determine protein

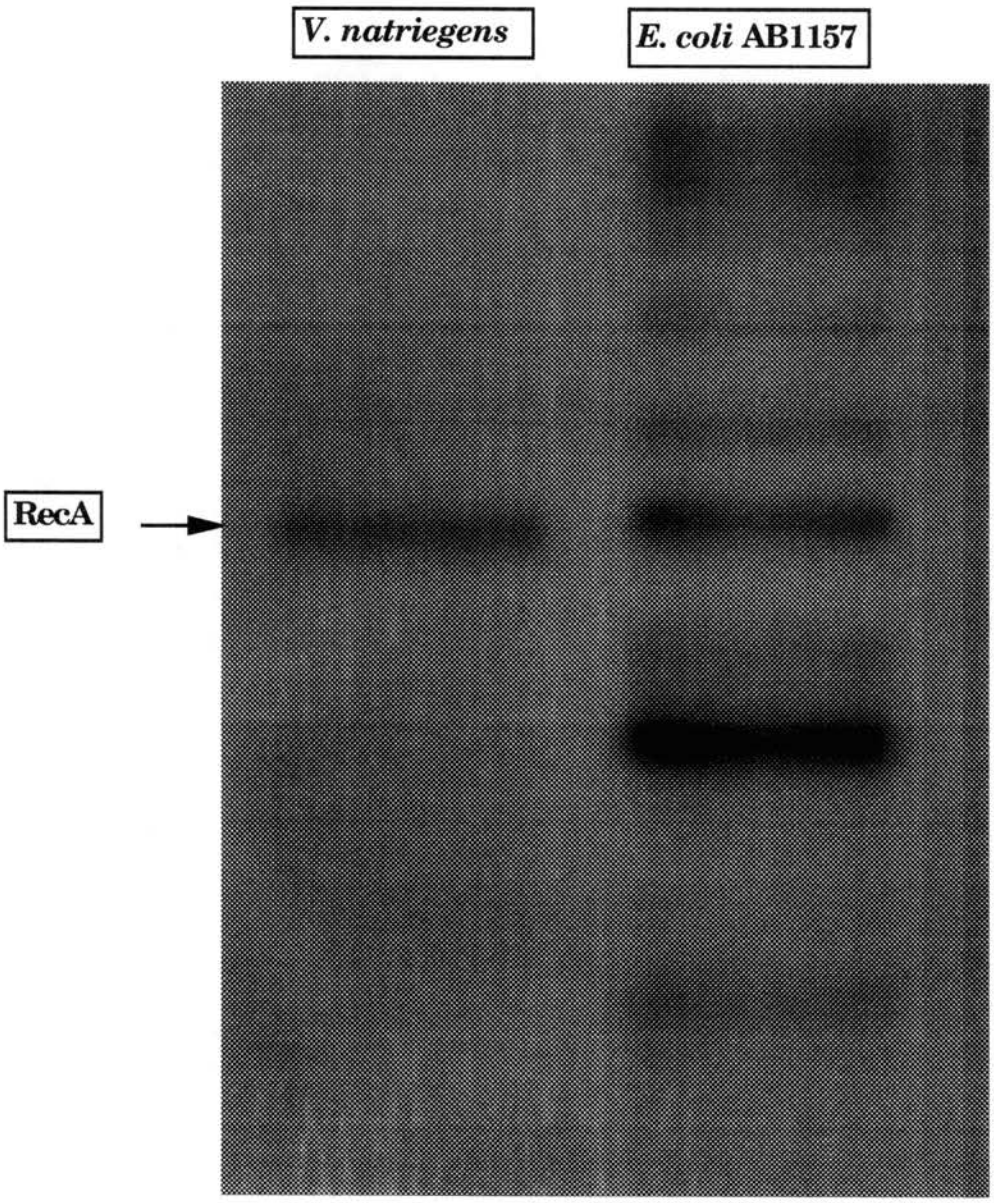

Fig. 3. Autoradiograph of Western blot testing *E. coli* anti-RecA antisera against total protein extract of *V. natriegens*. AB1157 was included as a positive control.

concentration using the BioRad DC Protein Assay Kit according to manufacturer recommendations (BioRad). Proteins were immobilized onto PVDF membranes by one of two methods tested. (1) Protein concentrations were adjusted to load 3-10 μg per well in gel-loading buffer (20% SDS, 10% glycerol, 5% ß-mercaptoethanol, 0.1% bromophenol blue, and 0.625M Tris pH 6.8) onto 12% SDS-PAGE gels. After separating the proteins at 100-150 volts for approximately 1.5 hours, the proteins were electrotransferred onto Immobilon™-P PVDF membrane (Millipore) with the BioRad Mini Trans-Blot cell as recommended by the manufacturer. (2) Alternatively, proteins were spotted onto a PVDF membrane using a Schleicher and Schuell slot blotter. A dilution series (5 μg/ml, 2.5 μg/ml, 1.25 μg/ml, 0.625 μg/ml, 0.3125 μg/ml) in 1X TBS (20 mM Tris, 500 mM NaCl, pH 7.4) or a specified concentration (either 2.5 μg/ml or 10 μg/ml) of protein was applied in 0.5 ml volumes to the membrane via the vacuum slot blotter. Membranes with immobilized proteins were analyzed by western blotting using the Immune-Lite™ kit (BioRad) according to manufacturer specifications. Primary antibody, *E. coli* RecA anti-sera generated from rabbit (Dr. Kowalscykowski) or mouse (OSU Hybridoma Center), was used a ratio of 1:5000 and incubated 4 hours as described above. After chemiluminescent development and autoradiography, the intensity of the reaction was quantified using a PDI laser densitometer model DNA 35 equipped with Quantity One version 2.2 software for the analysis of 1-D gels and dot/slot blots until 1996. Samples analyzed in 1996 and 1997 were quantitated with the Molecular Analyst Molecular Imaging System (BioRad) at the OSU Core Facility, Stillwater, OK. Densitometry allows quantification of the

amount of antigen-antibody complex as optical density (OD x mm x mm) units. Regression analysis was performed on the dilution series to establish a correlation between the protein signal and the amount of total protein in the cellular extract loaded on the blot. The signals were plotted individually against the amount of total protein loaded on the blot. The RecA signal (y axis) is related to the amount of total protein (x axis) in a lane by the linear regression equation $y = mx + b$ with a regression coefficient (r^2) of ≥ 0.9. This technique is useful for estimation of antigen levels (2). Quantities of samples that were not diluted were taken directly from the densitometric output.

DNA photoproducts. Analysis of DNA photoproducts was done by Dr. David Mitchell at the University of Texas MD Anderson Cancer Research Center in Smithville, TX as described by Mitchell et al. (47). Genomic DNA was isolated using a Wizard® Genomic DNA purification kit as recommended by the manufacturer (Promega). The samples were then quantified using a spectrophotometer according to standard protocols (ASM book) and mailed overnight frozen to Dr. Mitchell. He performed a radioimmunoassay (RIA) to measure the binding of radiolabeled UV-irradiated DNA to antibody raised in rabbits against triplet-sensitized, UV-B irradiated DNA. Briefly, a radiolabeled ligand was irradiated with 10 kJ/m^2 254 nm UV-C and added to a mixture of antiserum and sample DNA. DNA-bound antibodies were precipitated overnight at 4°C with goat anti-rabbit immunoglobulin and carrier immunoglobulin. After centrifugation, the pellet was solubilized with ^{32}P and quantified by liquid scintillation counting.

Under these conditions, antibody binding to an unlabeled competitor (sample DNA) results in reduced binding to the radiolabeled ligand (i.e. inhibition). Samples were compared to results obtained with standard DNA (e.g. pUC19) in which photoproduct formation is known (33).

UV irradiation. Polychromatic UV-R was generated by ultraviolet bench lamps (Spectronics Corp., Westbury, New York). Model XX-15N which produces a peak at 365 nm at approximately 1,200 $\mu W/cm^2$ at a 31 cm distance was used to generate UV-A. Model XX-15F which produces a peak at 254 nm at approximately 1,100 $\mu W/cm^2$ at a 15 cm distance was used to generate UV-C. Model XX-15B which produces a peak at 302 nm at approximately 1,800 $\mu W/cm^2$ at a 15 cm distance was used to generate UV-B. Measurement of irradiation was done with a UVX Digital Radiometer with different probes for each wavelength range (Ultra-Violet Inc., San Gabriel, CA). The spectra for the bulbs are represented in Figures 4, 5, and 6.

Monochromatic light was generated by a pulsed Alexandrite laser (Light Age model 101PAL), tunable over a wavelength range of approximately 720 nm to 780 nm. The laser operates at a pulse repetition rate of 20 Hz with each pulse being approximately 60 ms, henceforth called long pulses. Each long pulse is actually a packet of multiple, shorter pulses called pulseletts that have a pulse width on the order 90 ns. When the laser operates in the Q-switched mode, the pulses from the laser, henceforth called Q-switched pulses, are single pulses of light (versus the

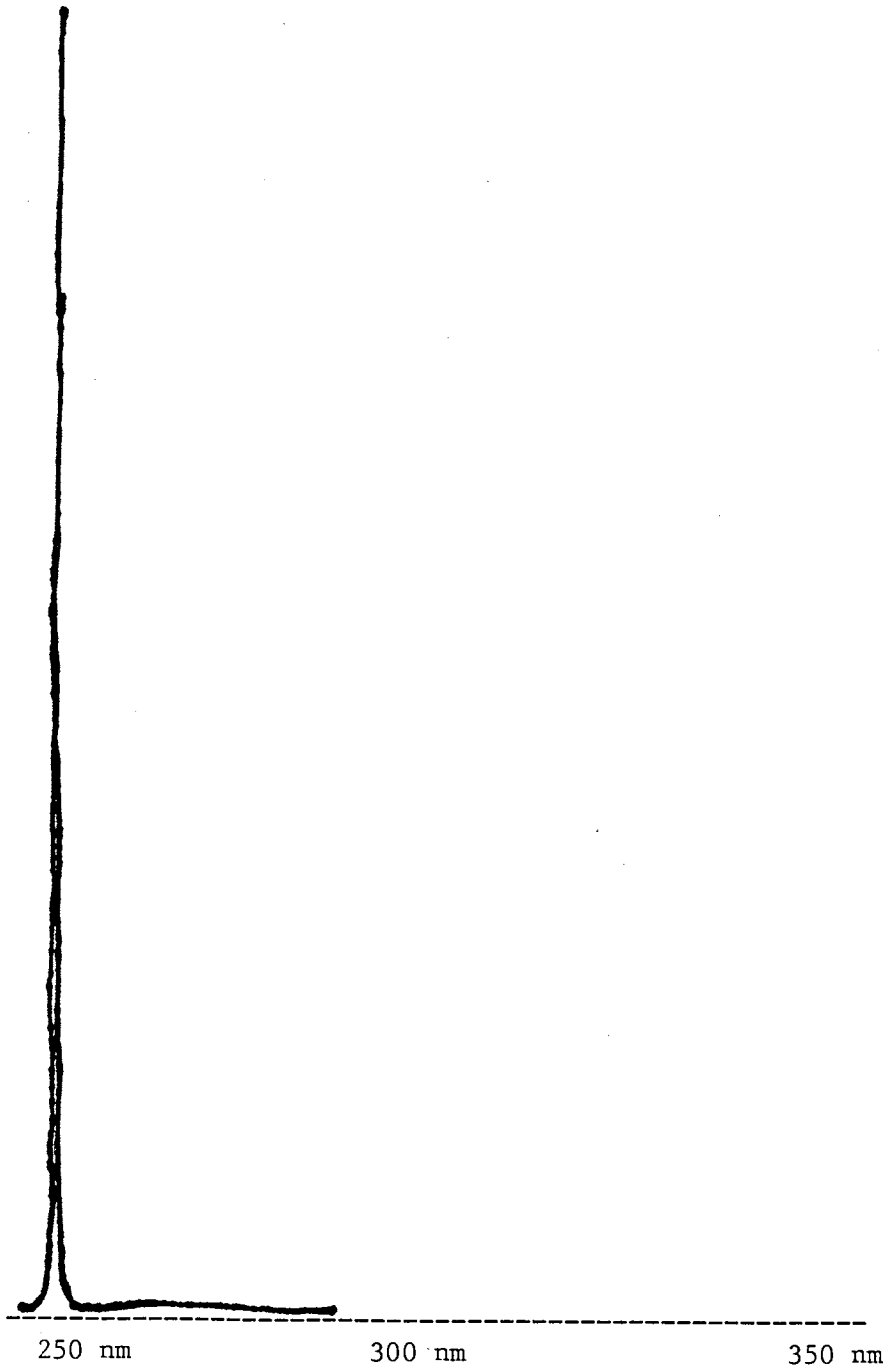

Fig. 4. UV spectra for bulbs used to generate UV-C light. Peak irradiance at 254 nm at approximately 1,100 μW/cm^2 at a 15 cm distance.

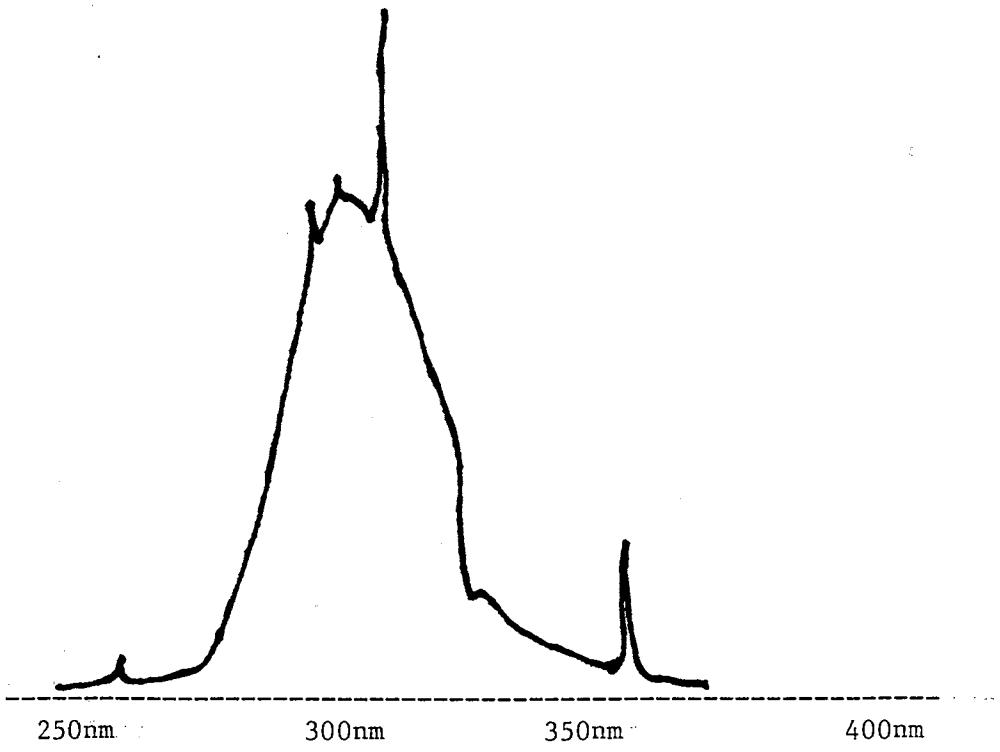

Fig. 5. UV spectra for bulbs used to generate UV-B light. Peak irradiance at 302 nm at approximately 1,800 μW/cm^2 at a 15 cm distance.

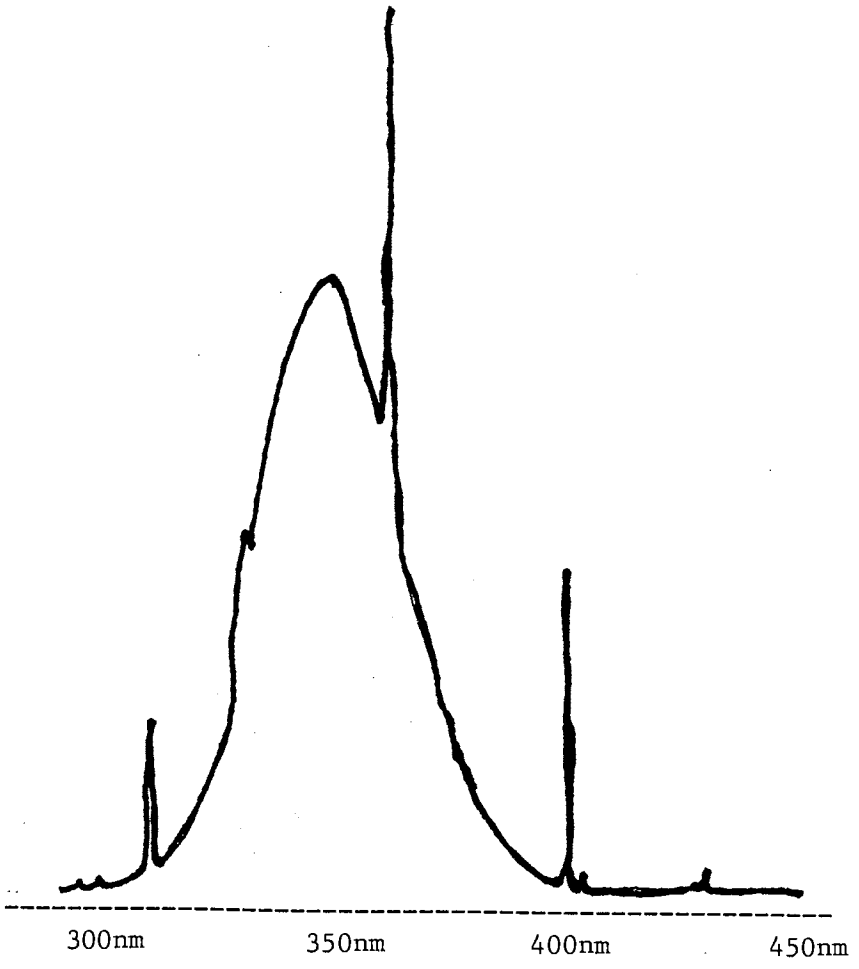

Fig. 6. UV spectra for bulbs used to generate UV-A light. Peak irradiance at 365 nm at approximately 1,200 μW/cm^2 at a 31 cm distance.

multiple pulses in long pulse mode) with a pulse width of approximately 90 ns.

Inside the laser cavity is a device known as a second harmonic generator (SHG). This device enables the wavelength of the laser to be halved, which in effect increases the energy of the light emitted from the laser. From the equation c = l n, where l is the wavelength of light, n is the frequency of light, and c is the speed of light, it is easy to see that doubling the frequency requires the wavelength to be halved to keep the speed of light constant. The energy of light is given by the equation E = h n, where E isthe energy of light, n is still the frequency of light, and h is Plank's constant, which shows that if the frequency doubles, the energy of the light doubles. So, if the laser is set at a wavelength of 720 nm, the second harmonic generator will convert that light to 360 nm.

In order to accommodate the laser, all the optics, the sample, and both detectors on one optics table, the setup required the "U" shape form as seen in the Figure 7. The beam exited the laser and was redirected to the opposite end of the optics table via two front-surface-coated mirrors (Virgo Optics). The beam from the laser is then passed through a Raman Cell filled with hydrogen gas at a pressure of approximately 300 psi (pounds per square inch gauge pressure). When the light from the laser interacts with the pressurized gas in the Raman Cell, the wavelength of the light is either Stokes shifted (increase in wavelength or decrease in energy) or Anti-Stokes shifted (decrease in wavelength or increase in energy). The light emitted from the Raman Cell is then directed through a prism to separate

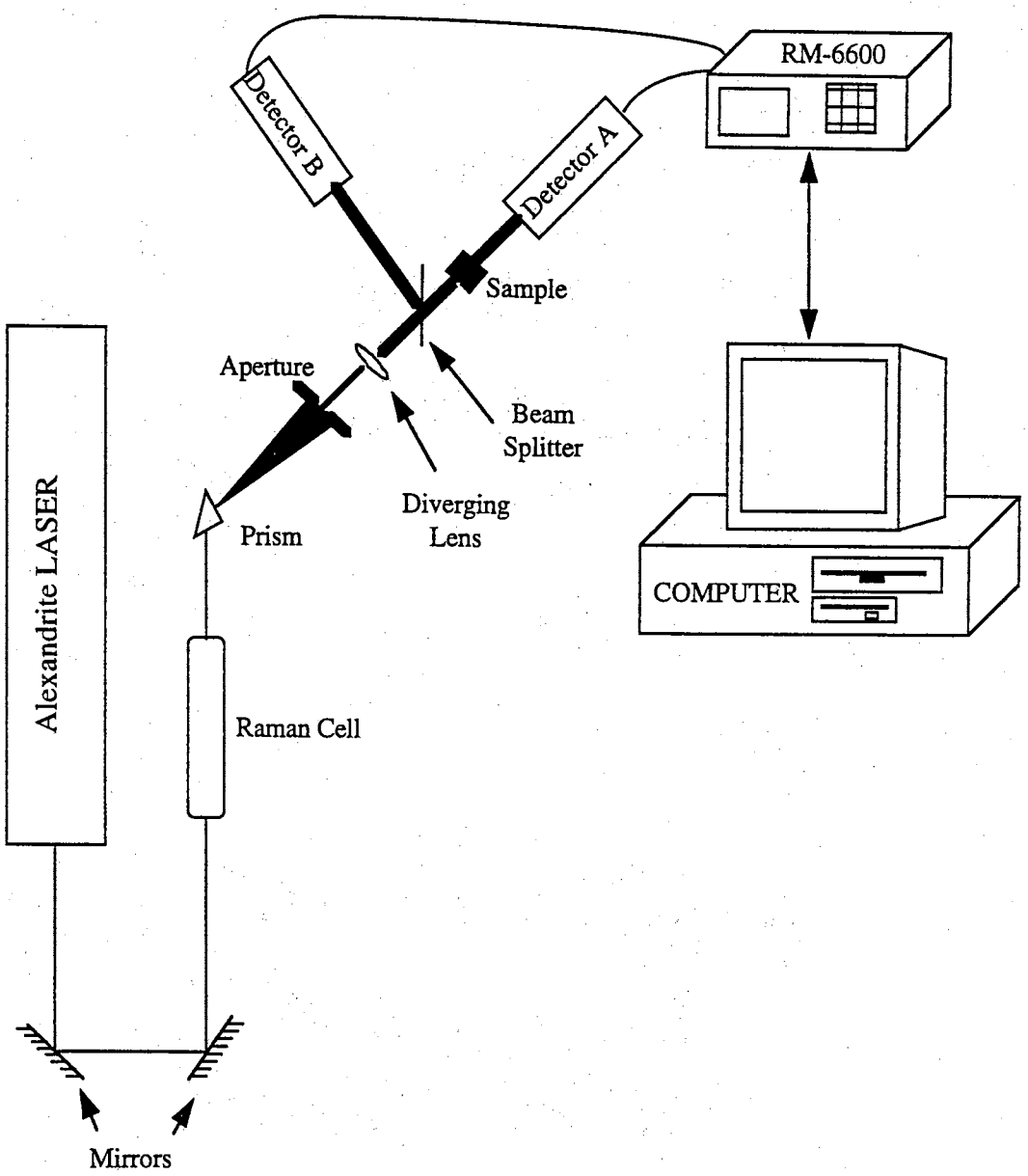

Fig. 7. Schematic diagram of set-up of Alexandrite laser

the shifted wavelengths. An aperture is then placed in front of the beam of separated light such that only one color of light is transmitted.

A diverging lens is placed in the path of this monochromatic beam of light to provide a larger spot size through the sample and on the surface of the detectors. The spot size on the sample was approximately 0.5 cm wide. To ensure a uniform distribution of energy deposition throughout the ICGsample, a miniature magnetic stirrer was placed inside the sample holder and driven by a Hellma CUV-O-STIR® (model 333).

The detectors used in the experiment were calibrated before each experiment due to the slight change in the setup every time a different color was selected for an experiment. The data from the detectors is then collected by computer, and displayed in real time on the computer monitor. The detectors (Laser Precision RJP-735) monitored the energy per pulse in real time. The energy meter (Laser Precision RM-6600) was connected to an IBM compatible 486 personal computer via a National Instruments NI-488.2 interface board. A computer program reads the data from the energy meter, displayed the real-time data on a computer monitor, and saved the data to a local hard disk. The data acquisition software was written in Microsoft QuickBasic Version 4.5 and was run under DOS 6.20. (The detailed description of the Alexandrite laser was generously provided by Jason Crull, OSU Physics Department).

In the environment solar irradiation was detected with a Biospherical PUV 500 profiling radiometer (San Diego, CA) within the water column and the surface. However, surface measurements were done with a GUV511C radiometer in Antarctica.

Various plastic filters were utilized in the environment to screen out various portions of the UV-R spectrum. Acrylite (50% transmission at 380 nm), is an acrylic resin made by Cyanid/Rohn and Cryo Industries (Fig. 8). Mylar, (50% transmission at 323 nm), is a poly (ethylene terepthalate) film or PET made by DuPont. Other uncharacterized plastics were obtained from Regal Plastics (Oklahoma City, OK). The absorbance spectrum for all materials used is shown in (Fig. 9).

Microbiological methods. Several standard microbiological methods were applied in this study and will briefly be described.

(i) Bacterial strains, plasmids, and bacteriophage. The bacterial strains, plasmids and bacteriophage used in this study are listed in Table 1.

(ii) Media and culture conditions. *V. natriegens* and other marine microorganisms were routinely grown in marine medium (MM) (DIFCO, Detroit Michigan) or Miller's Luria broth supplemented with 1.5% NaCl (LB 1.5% NaCl) (Gibco-BRL, Paisely, Scotland). Plates were made by adding agar to find a concentration of 1.3%. These organisms grew well both at room temperature and at 37°C. For phage studies, four salts nutrient medium (4SN) was used which contained 0.25 M NaCl, 3.8 mM KCl, 0.018 M $MgSO_4 \cdot H_20$), 3.8 mM $CaCl_2 \cdot 2H_20$ and DIFCO nutrient broth 10 g/L, DIFCO peptone 5 g/L, and DIFCO yeast extract 2.5 g/L. Bottom agar plates contained 1% agar and top agar was 0.6% agar.

(iii) Viable counts. Cells were diluted in 1.5% NaCl sterile saline by ten-fold dilutions. One tenth milliliter samples were spread-plated onto

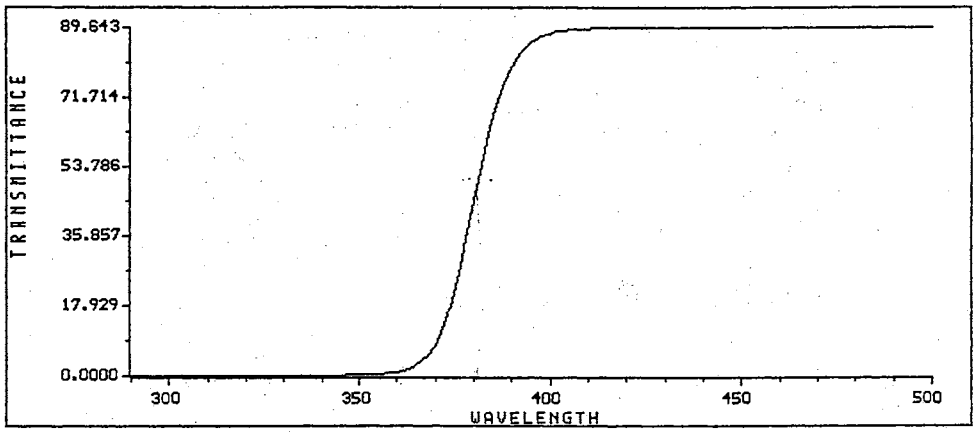

Fig. 8. Transmittance of wavelengths between 290 nm to 500 nm by Acrylite plastic material.

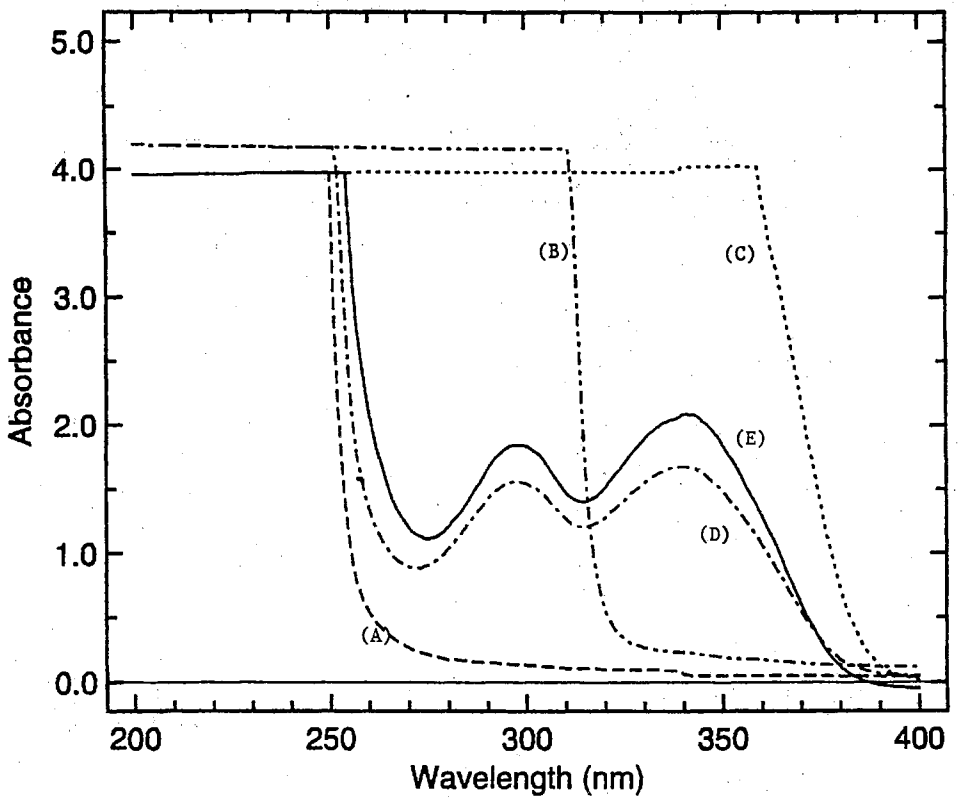

Fig. 9. Absorbance spectra of ultraviolet radiation of various plastic material. (A) OP-4, (B) Mylar, (C) Tanning Bed Insert (TBI), (D) Lucite, (E) Plexiglas UF-3. (D) and (E) were not used in this study.

Strain, plasmid or phage	Relevant genotype	Reference or source
Vibrio natriegens ATCC 14048	Wild-type	1
Vibrio natriegens ATCC 37088	Wild-type	1
Escherichia coli AB1157	*thr-1 leuB6 thi-1 proA2 his-4 argE3 supE44*	3
RM11001 Antarctic isolate	Wild-type	this study
RM11002 Antarctic isolate	Wild-type	this study
RM11003 Antarctic isolate	Wild-type	this study
pMETSK+	pBluescript®SK+ with *V. anguillarium recA*	4
pKT210	Mob+, Cm^r, Sm^r based on RSF1010	2
Phage nt-1	*V. natriegens* (virulent)	5
Phage nt-6	*V. natriegens* (virulent)	5

1. **Baumann, P., *et al.*** 1980. Curr. Microbiol. **4**:127-132.
2. **Bagdasarian, M*et al.*** 1981. Gene. **16**: 237-247.
3. **Clark, A.J., and A. D. Marguilies.** 1965. Proc. Natl. Acad. Sci. USA. **53**:451-459.
4. **Tomalsky, M.E.** 1992. Gene. **110**:41-48.
5. **Zachary, A.** 1978. Can. J. Microbiol. **24**:321-324.

Table 1. Bacterial strains, plasmids and bacteriophages used in this study.

either MM or LB containing 1.5% NaCl and incubated overnight at 37°C or room temperature.

(iv) DAPI. Total cell counts were done with modifications to Turley's procedure (59, 77). For bacterial enumeration 50 mls of 0.8 μm filtered seawater was fixed with 0.5 mls of Lugol's and stored up to 24 hours at 4°C. Samples were cleared with two drops of sodium thiosulfate. One milliliter of samples was filtered onto a Nucleopore polycarbonate black filter, stained with 4',6-diaminidino-2-phenylindiole (DAPI; final concentration, 1 μg/ml) (59, 77), placed onto microscope slides and stored at -20°C. Cells were counted using epifluorescence microscopy (Nikon Labophot-2 & 2A, Melville, NY).

(v) Survival studies. Bacterial sensitivity to UV irradiation was assayed as previously described (44). Cells were grown to logarithmic phase in MM or LB containing 1.5% NaCl to a concentration of 1 x 10^7 CFU/ml (60 to 80 Klett 660 nm units) and harvested by centrifugation at 6000 rpm in a Sorvall centrifuge. Cells were washed and resuspended in 1.5% NaCl. A portion of the suspension was placed into a sterile plastic petri dish (diameter, 10 cm) and exposed to various doses of UV-R. Survivors were determined by viable counts as described above. All manipulations subsequent to irradiation were carried out under amber light (Kodak Wraten OC) and incubated in the dark to prevent photoreactivation.

For studies utilizing the Alexandrite laser, 4 ml samples were placed into a cuvette specifically designed for this experiment by S. Schaefer (Edmond, Oklahoma) instead of a petri dish. During the laser

exposures, cells were mixed by placing a 7 mm magnetic stirbar into the cuvette and the sample was stirred over a magnetic stirplate. After each experiment the cuvette was rinsed with 95% EtOH and irradiated with UV-C overnight to sterilize it.

(vi) Chromosomal mutagenesis. It has been shown that organisms capable of carrying out SOS mutagenesis such as *E. coli* are mutable by UV-R and show increased frequency of rifampicin-resistant mutants following UV-C exposure. Rifampicin kills bacteria by inhibiting RNA polymerase and thus transcription. Resistance is acquired by alteration in the structure of the ß' subunit of RNA polymerase so that rifampicin no longer binds. After testing several concentration of rifampicin, *V. natriegens* was found to be highly sensitive to this compound and a concentration of 5 μg/ml was determined to be optimal for spontaneous mutation and selection. Cells exposed to various doses of polychromatic and monochromatic UV-R were grown under non-selective conditions on LB containing 1.5% NaCl to permit processing of DNA damage and expression of mutant phenotypes. After 12 hours, cells were replica plated as previously described (69) onto LB with 5 μg/ml rifampicin and allowed to grow 48 hours. Chromosomal mutagenesis was determined by calculating the number of rifampicin-resistant mutants per 1 x 10^6 survivors .

(vii) Weigle reactivation. Weigle reactivation is a measure of the inducible-DNA-repair capacity of the host cell (84). Briefly, lysates of a *V. natriegans* bacteriophage were irradiated (30 J/m^2 of UV-C) and diluted in 1.5% saline. One-tenth milliliter samples of UV-exposed and unexposed cells were mixed with various dilutions of the irradiated and unirradiated

lysates. Adsorption was allowed at room temperature for 15 min-1 h in the dark. The phage-adsorbed cells were added to 3 ml of 4SN top agar held at 42°C and poured onto 4SN plates and incubated at 37°C overnight. Plaques were counted and the Weigle reactivation factor (WRF) was calculated from the formula:

$$WRF = \frac{(PFU_{\text{øuv}}/PFU_{\text{øno uv}}) \text{ on irradiated host}}{(PFU_{\text{øuv}}/PFU_{\text{øno uv}}) \text{ on unirradiated host}}$$

$PFU_{\text{øuv}}$ is the titre of the irradiated phages and $PFU_{\text{øno uv}}$ is the titre of unirradiated lysate.

Laboratory UV-R experiments. The response of *V. natriegens* and RecA to UV-R was investigated under controlled conditions in the laboratory. For studies of the response to polychromatic radiation, cells were grown as described above. Ten milliliter saline-washed aliquots of *V. natriegens* were placed in plastic petri dishes and exposed to various doses of UV-R. After exposure all work was conducted under amber light to prevent photoreactivation. Samples of cells were taken prior to and after exposure. Samples for DNA photoproducts were taken directly before and after irradiation. DNA was extracted and analyzed for CPDs as described above. Viability and RecA protein was assayed prior to (T_0), directly after (T_1), one hour (T_2) after and two hours (T_3) after exposure. Chromosomal mutagenesis and Weigle reactivation were investigated as described above. For studies in response to monochromatic UV-R, samples were frozen after each experiment before analyzing in order to expediate usage of the Alexandrite laser. Samples were also taken at T_0, T_1, T_2 and T_3. DNA

Alexandrite laser. Samples were also taken at T_0, T_1, T_2 and T_3. DNA photoproducts, RecA induction, viability, chromosomal mutagenesis and Weigle mutagenesis were all investigated. Additionally, the generation of photoproducts in purified calf thymus DNA (Clontech, Palo Alto, CA) was investigated.

Environmental study sites. The pilot study for the environmental portion of this study was conducted aboard the RV BELLOWS in September, 1994 at approximately 29°N latitude and 87°W longitude in the Gulf of Mexico. The second study was done aboard the OSV ANDERSON in June, 1995. A third cruise aboard the RV LONGHORN in July and August, 1996 between 30°N to 20°N latitude and 95°W to 90°W longitude, further south than previous studies in the Gulf of Mexico. Additionally, studies were also conducted in October and November, Austral spring, of 1995 and 1996 in the Gerlache Straits, approximately 64 10 °N and 61 50 °W, Antarctica.

Experiments in the Gulf of Mexico. For the cruises in the Gulf of Mexico, acid-washed (10% HCl) 10 l Nalgene pans were placed in a water table with circulating seawater for temperature regulation. Eight liters of 0.2 μm filter-sterilized seawater was placed into each tub and inoculated to approximately 1 x 10^8 cells/ml with a dense overnight culture of *V. natriegens*. Previously, growth curves of *V. natriegens* were done to determine the maximum cell densities possible, as well as doubling times (Fig. 10). The microcosms were covered with various plastics to filter various segments of the solar UV spectrum. Samples were withdrawn from the tanks with sterile plastic pipettes periodically. For the study

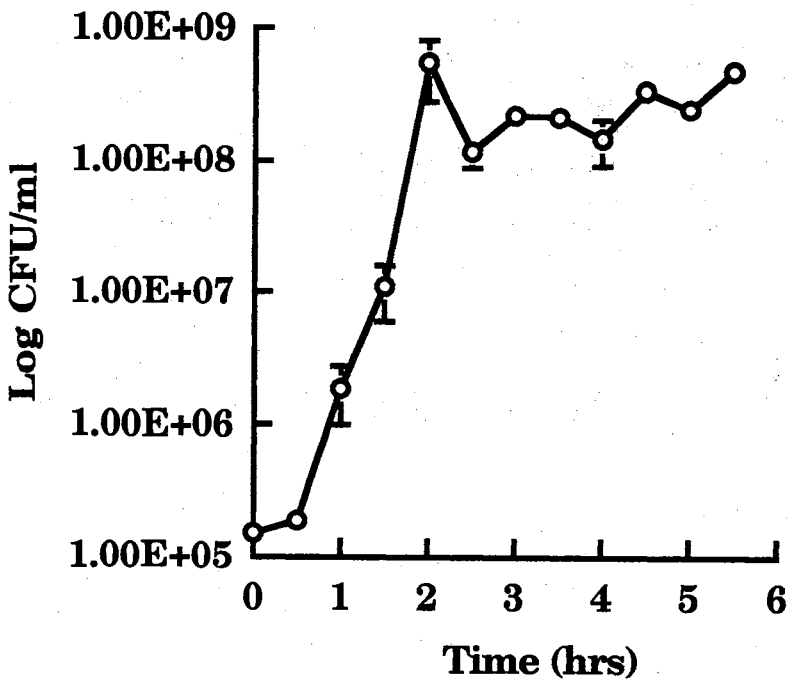

Fig. 10. Growth curve of *V. natriegens* in MM at room temperature. 11.5 generations turned over with a doubling time of approximately 28 minutes.

aboard the RV BELLOWS, samples were treated in three ways: [1] Serial dilutions and spread-plating as described above was done to measure survival, [2] 10 ml was filtered onto 0.2 μm, pore-size, 25 mm discs and frozen for later measurement of RecA protein, [3] 10 ml was filtered onto 0.2 μm, pore-size, 25 mm filter discs for later measurement of DNA photoproducts. However, samples obtained by filtration for RecA protein and DNA photoproducts in 1994 proved difficult to analyze due to low amounts of sample material. Therefore in 1995 duplicate 10 ml samples in sterile polypropylene tubes for both RecA protein and DNA photoproducts were obtained by harvesting cells in a clinical centrifuge at full speed 20-30 minutes and freezing the cell pellet at -80°C for later analysis.

In 1996, attempts were made to eliminate contamination from the experiments for ease of analysis. Although high densities of *V. natriegens* within the microcosms kept contamination to a minimum, microcosms left open to full sunlight were often contaminated with foreign objects and low but detectable numbers of other microorganisms. *V. natriegens* was tested for streptomycin resistance. The organism was found to be inhibited by concentrations higher than 60 μg/ml but only limited at lower concentrations and unaffected at concentrations below 25 μg/ml. Electrocompetent cells were prepared as described by the Electrocell manipulator®600 electroporator manufacturer (BTX Corp., San Diego, CA). 1 μg/ml of pKT210 DNA which encodes streptomycin resistance was electroporated at 12.5 KV, 5 ms, 200 Ω resistance, and 25 μF capacitance with electrocompetent *V. natriegens* cells. Recovery was done in SOC containing 1.5% NaCl for 3 h at room temperature. However, a streptomy-

cin resistant transformant was not established. Therefore, an effort was made to physically eliminate contamination in the microcosms receiving the full solar spectrum with an additional plastic light filter (OP-4, Fig. 9).

Additional experiments to investigate survival at different depths, recovery capability and photoreactivation in *V. natriegens* were executed in 1996. These were done in Whirlpak® (Nasco) bags instead of the larger microcosms to facilitate many samples. Twenty-five milliliter of 0.2 μm filter-sterilized sea water was placed into several Whirlpak® bags (100% transmittance of UV-B) (37) and was inoculated at a final concentration of 1×10^8 cells/ml with *V. natriegens*. Triplicate bags were covered with each of the various plastics and either placed into the ocean attached to a deployment array, or placed into the circulating water table. Samples were removed from the bags periodically to determine viability and RecA protein concentrations.

Experiments in Antarctica. Seawater samples for RecA analysis of natural bacterioplankton in 1995 and 1996 were prefiltered through a 0.8 μm filtration unit and then filtered onto 0.2 μm filter discs and frozen at -80°C. Total cell counts were done as described above (DAPI).

Isolation of natural Antarctic strains was done in 1996 to conduct similar experiments as previously done in the Gulf of Mexico. International regulations prohibit the use of isolated laboratory strains in Antarctica, thus *V. natriegens* was not taken for use. Three microorganisms were isolated on media containing autoclaved sea watercontaining 1.5% agar (DIFCO) and 0.05% Casamino acids (DIFCO) and 0.05% Bacto-Peptone (DIFCO). Two of these isolates were used for controlled experiments

similar to those conducted in the Gulf of Mexico. Whirlpak® bags containing 0.2 μm, pore size, filter- sterilized seawater were inoculated to an optical density of 0.6 with overnight cultures of the selected Antarctic isolate, RM 11001 (Table 1). Three samples were placed under each of the various plastics and sampled for RecA protein and cell survival periodically. Viable cells were enumerated as previously described. Total cell numbers were also counted utilizing the DAPI method described above. An additional experiment was conducted to investigate photoreactivation and recovery capacity as described on the Longhorn cruise in the Gulf of Mexico 1996.

The Antarctic bacterial isolates were found to be Gram-negative aerobes capable of surviving within a wide temperature range on various rich media. PCR and sequence analysis utilizing the *E. coli recA* as a probe showed that these organisms do have a *recA* gene and belong to the purple bacteria of the gamma subdivision. BIOLOG (BIOLOG, Inc., Hayward, CA) analysis indicated similar results. However, BIOLOG analysis is aimed at identifying human pathogenic bacteria. BIOLOG results were inconclusive, but do indicate the Antarctic isolates, RM 11001, RM 11002, and RM 11003 are members of the purple bacteria of the gamma subdivision.

CHAPTER IV

RecA EXPRESSION IN RESPONSE TO SOLAR UV-R IN MARINE BACTERIA

Introduction

Over the past two decades results of several studies have confirmed a decrease in Earth's protecting ozone layer resulting in increased UV-R penetration to the surface (14, 16, 20, 53, 63, 70, 72, 81, 89). Bacteria in the marine environment have been shown to be significantly impacted by UV-R (1, 4, 18, 21, 22, 34, 35, 78). Questions have been raised on how increased UV-R penetration may affect various food webs and geochemical cycles in the marine environment.

With limited physical defenses against UV-R, bacteria employ several repair mechanisms to counteract UV-R-induced DNA damage they experience. Damages may include cyclobutane pyrimidine dimers (CPDs), 6,4 pyrimidine pyrimidones (6,4PDs), or Dewar photoisomers (12, 32, 33, 46, 48, 49, 61, 62). Several studies have indicated that photodependent repair processes play the decisive role in bacterial recovery after UV-R stress (17, 36, 41, 52, 85, 87). However, results of this study

indicate other repair mechanisms involving RecA are also important to bacterial recuperation.

This study was conducted using a model marine microorganism, *V. natriegens*, which is ubiquitous in marine environments. Inherent variability is encountered when studying natural communities. Responses and interactions of a mixed plankton community at various trophic levels are highly complex at the ecological and molecular levels. By examining responses of an isolated microorganism, specific questions about members of the marine bacterioplankton community can be answered without trying to interpret or infer unknown interactions with higher trophic levels.

Results and Discussion

Effect of solar UV-R on bacterial viability. To investigate the survival of our model microorganism after solar UV assault, microcosms were constructed on the deck of various research vessels in attempts of mimicking a surface environment while observing one organism. The pilot study in 1994 demonstrated that the viability of*V. natriegen's* was significantly impacted by UV-R (Fig. 11). This experiment was done to demonstrate how the ultraviolet portion of sunlight affects a marine bacteria. Microcosms containing *V. natriegens* were exposed to full sunlight, left unexposed, or covered with an acrylic filter to screen out UV-R. In 1995, a

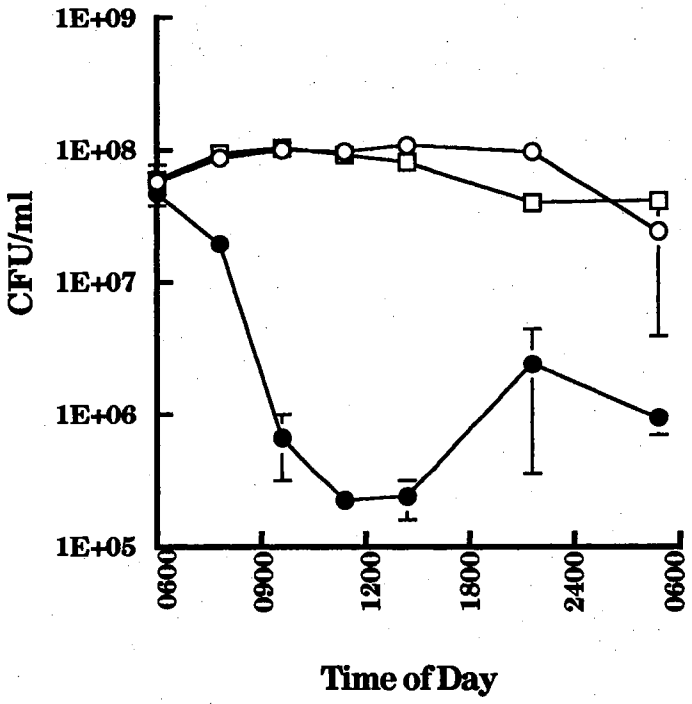

Fig. 11. Survival of *V. natriegens* over 24 h after exposure to solar UV-R in *in situ*-mimicking experiments conducted in 1994. Microcosms underwent the following treatments: unexposed (open circles), exposed to full sunlight (closed circles), and UV-R-filtered sunlight using an acrylic screen (open squares).

Mylar filter was added to differentiate between effects of total solar UV-R and solar UV-A. Additionally, experiments were extended to 48 h to observe cyclic patterns in cell recovery or protein induction. Weather patterns for the first 48 h experiment were continuously partially cloudy whereas clear skies prevailed throughout the course of experiment 2. Remarkably similar results were observed for both experiments and are averaged together to provide information comparable to natural marine communities experiencing daily weather changes. Viability was significantly decreased by the evening of the first day in the microcosms receiving full sunlight and UV-A (Fig. 12). This indicates that UV-A is the portion of the solar spectrum responsible for loss of viability as previously suggested (24). A recovery of cell numbers was observed by the following morning as in 1994 (Fig. 12). On the 2nd day an evening decline and subsequent overnight recovery was again observed (Fig. 12). This may indicate a cyclic pattern in accumulation of UV-R induced damage and repair. In 1996, cultures were inoculated at higher densities than previous experiments to increase sample concentration. As observed in 1994 and 1995, viability was decreased late in the day in microcosms receiving full sunlight and UV-A though to a lesser degree than previously observed (Fig. 13). Higher CFU/ml aided in obtaining more protein and DNA for analysis. However, this may have had a shading affect within the microcosm resulting in a higher rate of survival and less inhibition than observed in 1994 and 1995. UV-flux was not significantly different than previous years (values of incident surface irradiance and penetration

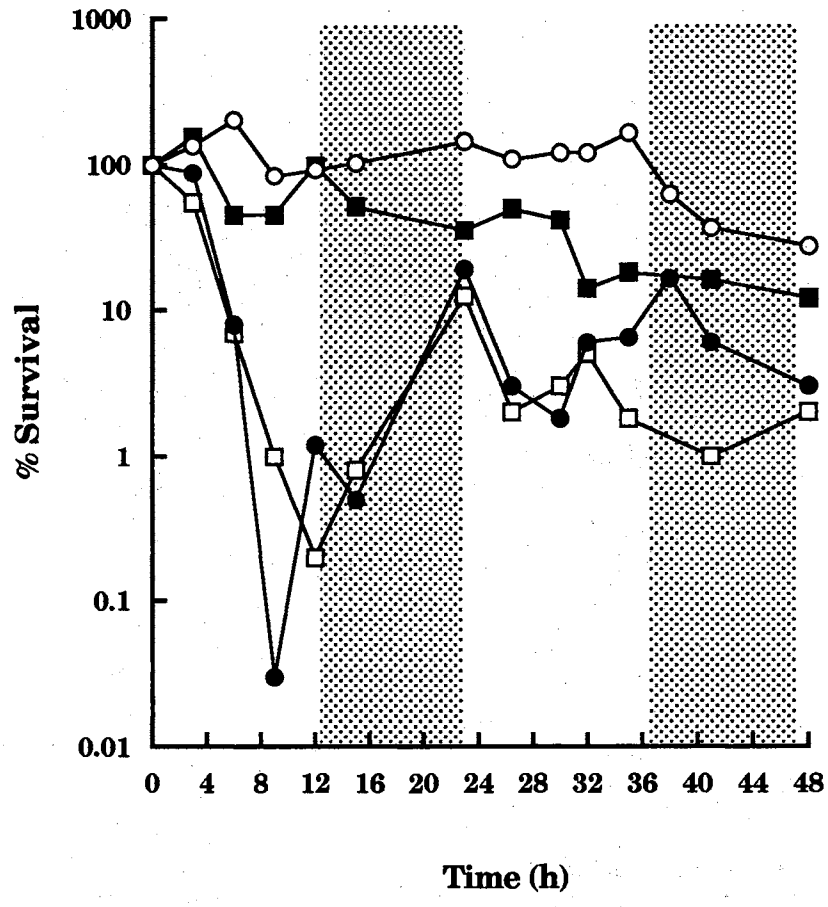

Fig. 12. Survival of *V. natriegens* in *in situ*-mimicking experiments exposed to different wavelengths of the solar UV-R spectrum. Experiments were initiated at sunrise. The shaded areas indicate the evening (dark) periods. Microcosms underwent the following treatments: unexposed (open circles), full sunlight (closed circles), UV-B-filtered sunlight using a mylar screen (open squares), and UV-R-filtered sunlight using an acrylic screen (closed squares).

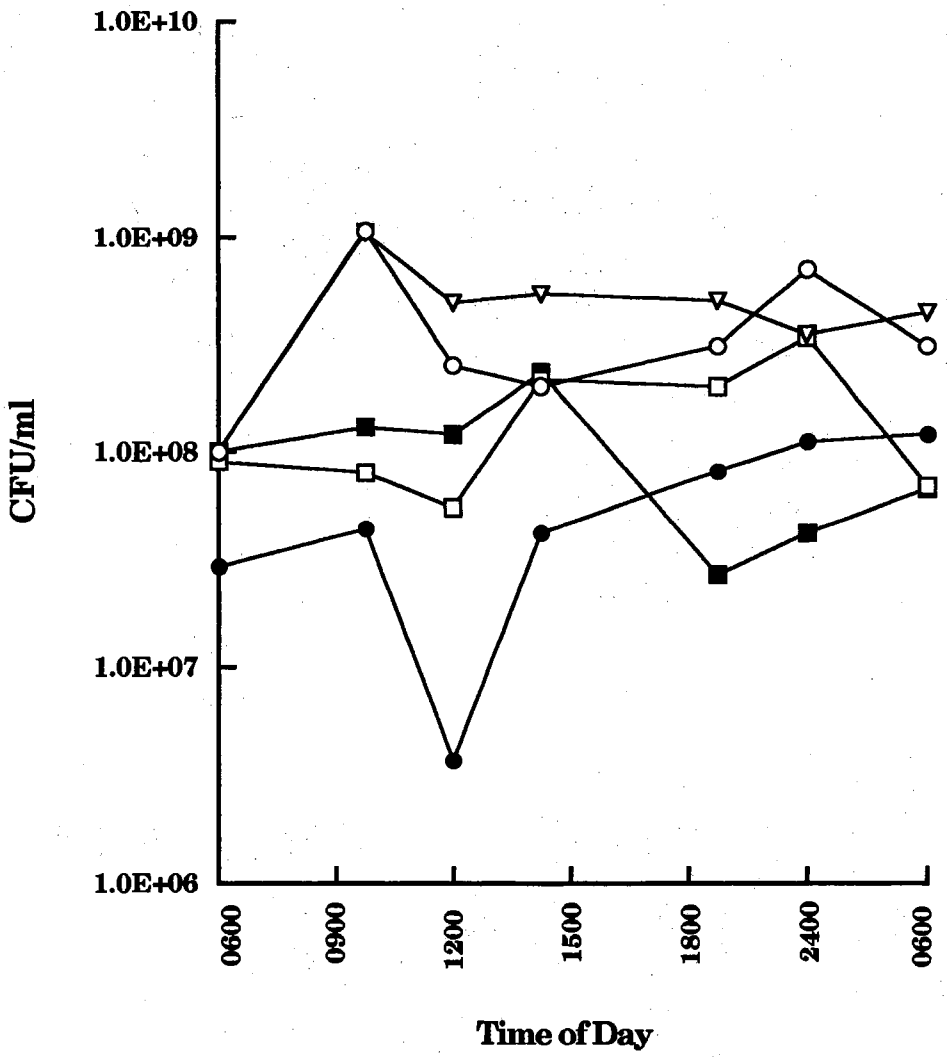

Fig. 13. Survival of *V. natriegens* in *in situ*-mimicking experiments conducted in 1996 exposing cells to different wavelength ranges of the solar UV-R spectrum. Microcosms underwent the following treatments: Unexposed (open circles), full sunlight (closed circles), UV-B filtered with mylar screen (open squares), UV-R filtered with acrylic screen (closed squares), and UV-R and PR (photoreactivating light) filtered with an amber screen (open triangles).

through the water column in the Gulf of Mexico for these cruises has been published elsewhere (34,35,85)). Weather patterns in 1996 were partially cloudy for experiment one and clear for experiment two.

Table 2 demonstrates loss of viability by *V. natriegens* at varying depths. One percent light penetration for 305 nm light was 24 m and 128 m for 380 nm light. The light attenuation (Kd) values were 0.147 for 305 nm, 0.099 for 320 nm, 0.064 for 340 nm, 0.047 for 340 nm, and 0.065 for 380nm. The value for photosynthetically active radiation (PAR) was 0.044 Kd. We can clearly observe that cultures at the surface and 5 m were significantly inhibited. Cultures placed at 10 m depths did not show a loss of viability, but failed to thrive as the control and 15 m cultures. There are two likely explanations for this observation; (1) arrested growth and/or (2) DNA damage and repair ratios. At 10 m attenuation of UV-B favors a higher ratio of UV-A to UV-B. Researchers have suggested that this ratio decreases the incidence of UV-R-induced damage and allows photodependent repair which utilizes wavelengths int he UV-A range creating an equilibrium between damage and repair. If damage repair is occupying the cell's replication system as well as depleting available energy resources, it is reasonable to suggest a resulting growth delay. However, photodependent repair mechanisms are specific for repairing lesions normally produced by the shorter wavelengths of the solar spectrum. For my experiment, this observation is important as the cells were maintained at a fixed depth throughout the experiment which may have prevented significant amounts of these lesions from forming as would be seen in a mixed community. Additionally, one must keep in mind that

Depth	Number of Cells CFU/ml	Percent survival or increase at sunset
Control	8×10^9	2000
Surface	2×10^7	5.00
5 m	7×10^6	1.75
10 m	5×10^8	125
15 m	5×10^9	1250

Table 2. Survival of *V. natriegens* after a full day of sunlight at various depths within the water column in the Gulf of Mexico in 1996. Samples of *V. natriegens* at an initial concentration of 4×10^9 CFU/ml were placed in Whirlpak® baggies, attached to a deployment array, placed in the water column at sunrise, and retrieved at sunset. Control cultures were covered with black plastic and placed in an on-deck circulating-seawater table for temperature regulation.

high doses of UV-A such as those found at 10 m also results in significant cellular damage which is not repaired by photodependent mechanisms. Many studies speculate that an intermediate molecule, such as heme, flavin, or bilirubin absorbs the incident UV-A photon and transfers the energy to DNA (9). Other studies have shown that thiolated tRNA molecules are inactivated by UV-A (32, 55). UV-A produces a crosslink of the 4-thiouracil with cytosine, thus inactivating the acetylation capacity of these tRNAs. This inactivation leads to abrupt cellular growth delay and reduction of cell size. But, on the other hand, UV-A can induce lesions which are repaired by photodependent enzymes (6,4 photolyases). From my data, bacteria existing at 10 m depth experience arrested growth due to UV-A-induced damage or high rates of DNA repair of UV-B and UV-A-induced lesions. We observed growth in cultures existing at 15 m depth similar to our dark controls. UV-B is significantly attenuated at this depth whereas UV-A is not. This suggests that the static growth observed at a 10 m depth was the result of an equilibrium of DNA damage accumulation and DNA repair processes within the bacterial cells.

The recovery of bacteria after solar UV-R exposure in the presence and absence of continued solar radiation was explored. Previous reports have shown higher amounts of infective bacteriophages and bacterial productivity in the presence of photoreactivation-inducing wavelengths (36, 85). Dark repair is often overlooked, but has been shown to be active (34). Fig. 14 presents data on dark-repair in cultures which were exposed to solar-UV-R and then allowed to recover in (1) full sunlight, (2) dark, (3) visible light >450 nm and (4) UV-B filtered sunlight for 3 h. Cultures were

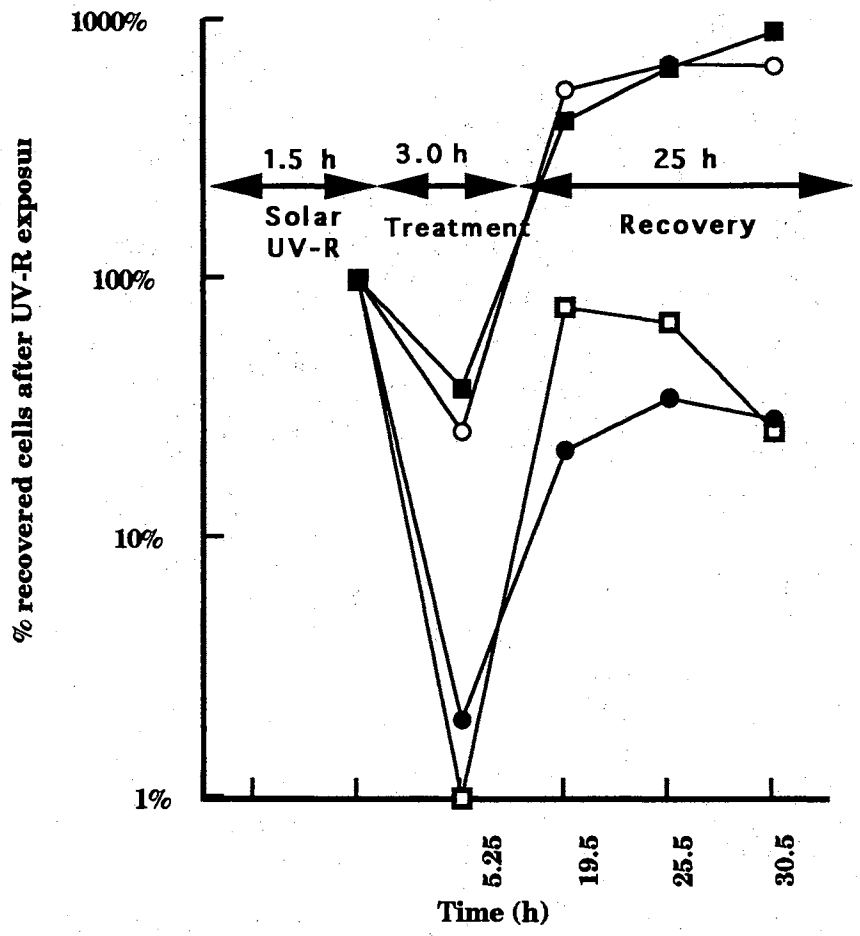

Fig. 14. Recovery of solar UV-R exposed *V.natriegens* in the presence and absence of solar UV-R. Initial exposure of bacterial cells for 1.5 hours to midday solar UV-R resulted in 90% loss of viability. Cells were shifted to different treatments for 3 h and then placed in the dark. Results indicate % survival relative to the amount at beginning of treatment. Treatments after initial exposure were dark (open circles), full sunlight (closed circles), UV-B-filtered sunlight with a mylar screen (open squares), and UV-R- and PR-filtered sunlight with a plastic TBI screen (closed squares).

then placed in the dark and sampled for 24 h. Exposure of a *V. natriegens* culture at a concentration of 1x 10^6 cells per milliliter of media to solar light for 1.5 h resulted in 90% loss of viable cells. A further decrease in viability was seen in all cultures after 3 h treatment, though to a greater extent in cultures receiving additional sunlight or UV-A (Fig. 14). As an aside, this significant mortality in less-dense cultures of *V. natriegens* corroborates the observation that microcosms in the 1996 study inoculated at high cell densities demonstrated higher rates of survival. This is likely a result of the increased cell numbers shading (Fig. 14). From this experiment, I observed that visible light does not affect cell viability (Amber filter). Cells denied photoreactivating wavelengths after solar UV-R exposure recovered viability indicating that dark-repair mechanisms significantly repaired damage. Cells exposed to solar radiation or UV-B-filtered radiation after the initial treatment demonstrated $\geq$95% greater loss of viability. This indicates again that UV-A is sufficient to reduce cell numbers whether large amounts of UV-B are present or not. The higher rate of recovery in cells treated with UV-B-filtered light indicates that dark-repair mechanisms may be more efficient at repairing damage induced by the longer wavelengths. This would agree with studies that show RecA binds more efficiently to 6,4PD photoproducts than cyclobutane dimers (61).

Induction of RecA by solar UV-R. In 1994, RecA protein induction in *V. natriegens* was observed at detectable levels after exposure to solar UV-R (Fig. 15). In 1995 similar results were observed (Fig. 16). Levels of induction in cultures receiving UV-A and UV-B compared to those receiving only UV-A were comparable indicating that RecA is likely responding to a

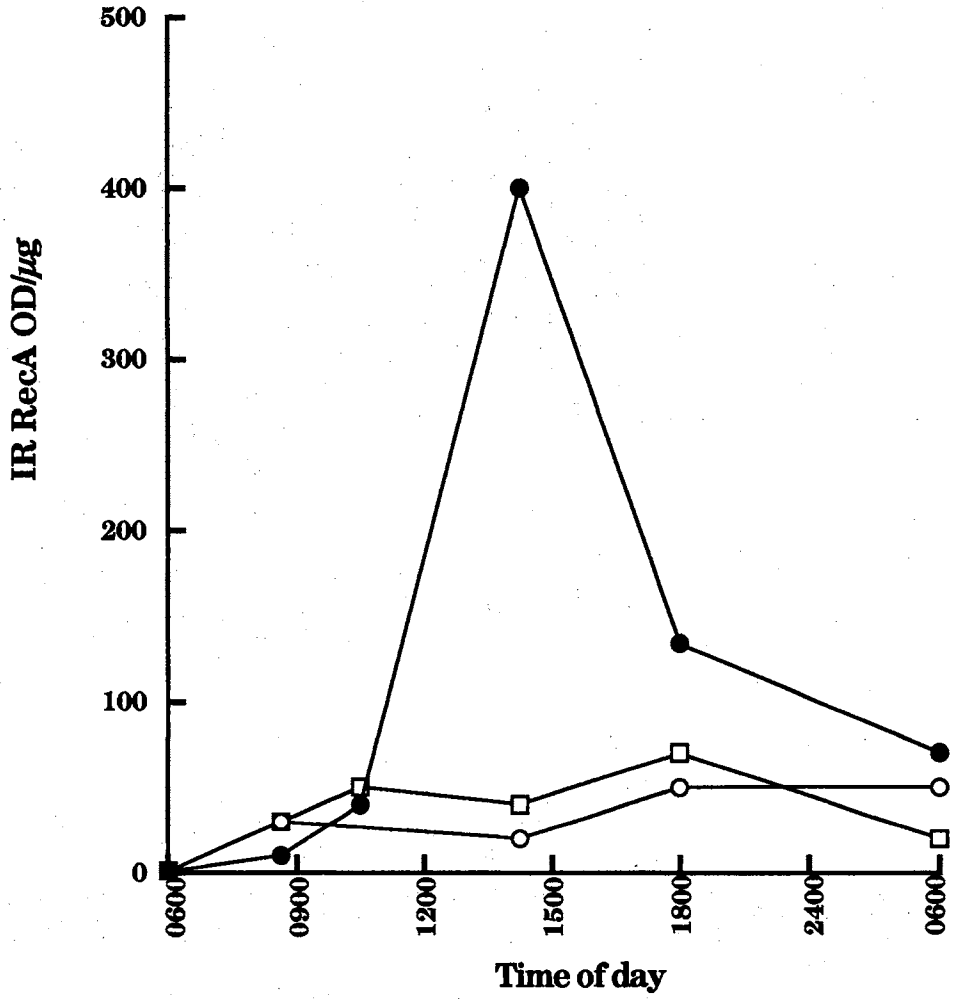

Fig. 15. RecA protein induction in *V. natriegens* in experiments conducted in 1994. Protein extracts of *V. natriegens* samples taken every 4 h over 24 h from *in situ*-mimicing microcosms were analyzed by SDS-PAGE and Western analysis to determine the amount of RecA protein expression. IR is the relative amount of RecA expressed in optical density units (OD) per µg of total protein extract at each timepoint compared to the amount at the beginning of the experiment. Microcosms underwent the following treatments: unexposed (open circles), exposure to full sunlight (closed circles), and UV-R-filtered sunlight using an acrylic plastic filter (open squares).

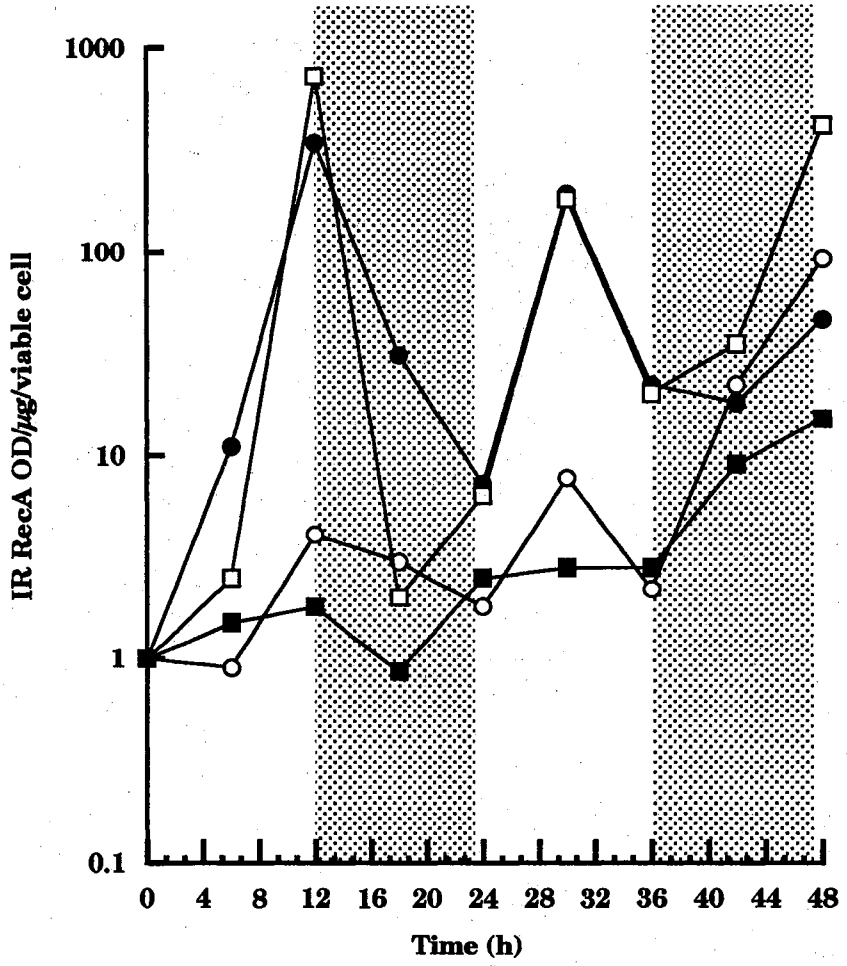

Fig. 16. RecA induction in *V. natriegens* in *in situ*-mimicking experiment conducted in 1995. Two experiments were conducted. This graph represents data from one conducted on a sunny day, although both look very similar (data not shown). Samples for protein extraction were taken periodically for 48 h from microcosms containing *V. natriegens* cultures. Experiments were initiated at sunrise. The shaded areas indicate the evening (dark) periods. Microcosms underwent the following treatments: unexposed (open circles), full sunlight (closed circles), UV-B-filtered sunlight using a mylar screen (open squares), and UV-R -filtered sunlight using an acrylic screen (closed squares). Improved technique was used in 1995 for sample analysis. Therefore IR RecA is the OD per μg total protein per viable cell. Protein analysis was done by serial dilution slot-blots and Western blotting.

UV-A- induced lesion. Over 48 h RecA levels increased toward the end of the daylight period and rapidly decreased again in both the UV-B filtered and UV-R filtered microcosms (Fig. 16). A similar cyclic phenomenon was previously noted in dimer accumulation among natural populations receiving solar UV-R with peak levels occurring after sundown (34). However, RecA induction does not appear to be a function of T<>T formation (see below).

As mentioned earlier, microcosms were inoculated at a higher concentration in the 1996 studies. Viable counts demonstrate that this procedure had a protective effect most likely due to shading. Only those test chambers receiving full sun showed a decline in cell numbers and increase in RecA production (Fig. 17). This indicates that although experiments in 1995 indicate that RecA is responding to a UV-A induced lesion, UV-B may be partially responsible for inducing this enzyme as well. Furthermore, RecA induction was observed several hours after sundown in the UV-B- and partial UV-A-filtered microcosms in both experiments done in 1996. This response may have been below the limit of detection in previous surveys as cultures were obviously impacted differently. Shading resulted in the cells receiving lower total doses of UV-R received per cell. In microcosms receiving full sunlight, the combination of UV-B and UV-A wavelengths, though at lower doses, was still sufficient to elicit RecA induction. In contrast, UV-B-filtered cultures were able to cope with the lower doses of UV-A. Significant changes in viability were not observedThis does not disclude previous results which demonstrate UV-A severely impacts bacterial populations (23, 24, 25). Merely, the

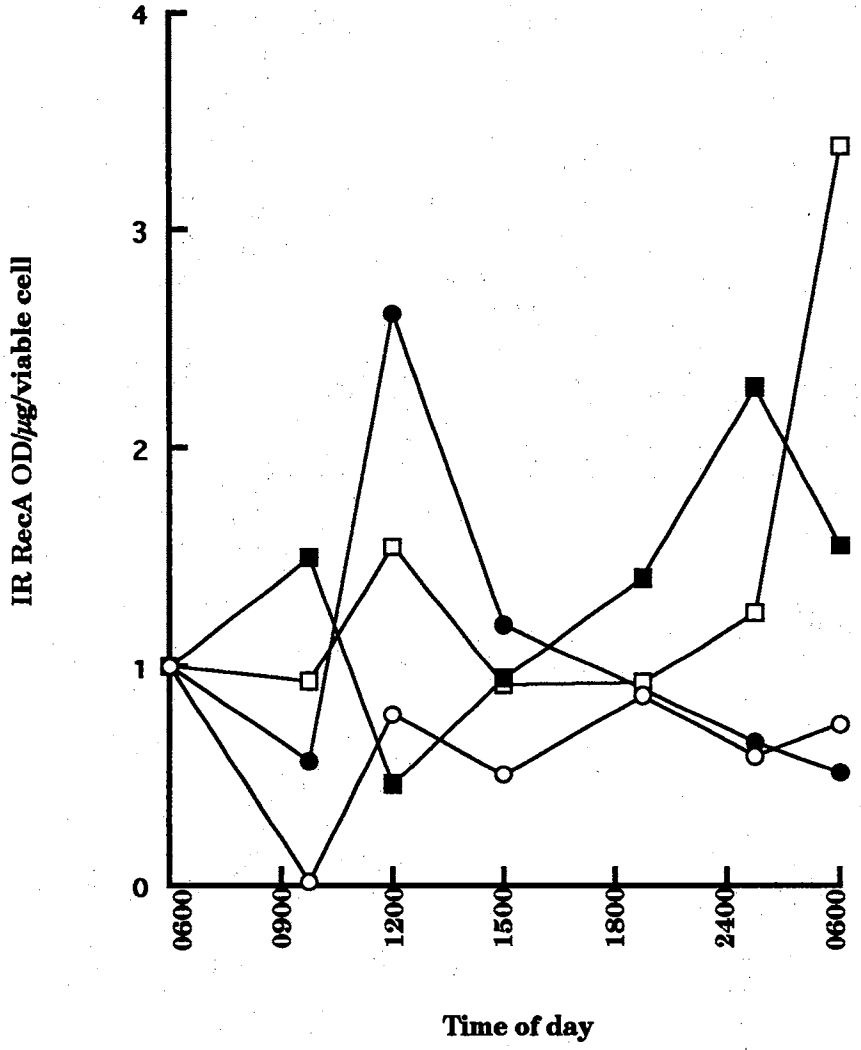

Fig. 17 . RecA induction in *V. natriegens* in *in situ*-mimicking experiment conducted in 1996. This graph represents one experiment conducted on a sunny day. Samples for protein extraction were taken periodically over 24 h from microcosms containing *V. natriegens* cultures. The experiment was initiated at sunrise. Microcosms underwent the following treatments: unexposed (open circles), full sunlight (closed circles), UV-B-filitered sunlight using a mylar screen (open squares), and UV-R <360 nm-filtered sunlight using a TBI screen (closed squares).

cope with the lower doses of UV-A. Significant changes in viability were not observed. This does not disclude previous results which demonstrate UV-A severely impacts bacterial populations (23, 24, 25). Merely, the unforeseen complication of shading has provided a useful observation about RecA responding to sub-lethal doses of UV-A. In a previous review of UV-induced damages, Eisenstark (12) presented the case for lesions produced by sub-lethal doses of UV-A. Often these wavelengths are absorbed by an initial chromophore and this energy is then transferred to DNA causing damage. However, this process takes time. The delayed induction of RecA in the UV-B-filtered microcosms is most likely due to damage induced by sub-lethal doses of UV-A. These data support the observation in RecA is responding a great deal to lesions induced by UV-A.

Formation of cyclobutane dimers. Jeffrey et al. (34) have demonstrated that bacterioplankton in unmixed surface layers accumulate significant amounts of DNA photoproducts (i.e. T<>T dimers) in response to solar UV-R. This effect was investigated in our model to elucidate a relationship between T<>T accumulation, cell viability and RecA induction. The pilot study in 1994 was encouraging as T<>T dimers were shown to accumulate like RecA in microcosms receiving sunlight (Fig. 18). However, in 1995 the inclusion of the Mylar filter to screen UV-B and the extended-length of time over which the study was conducted clearly demonstrated that RecA induction is not related to T<>T dimers (Fig. 19). On day 1 of the study conducted in 1995 accumulation of dimers was only observed in microcosms receiving full sunlight, whereas RecA induction was also observed in tanks receiving UV-B filtered sunlight. The most significant accumula-

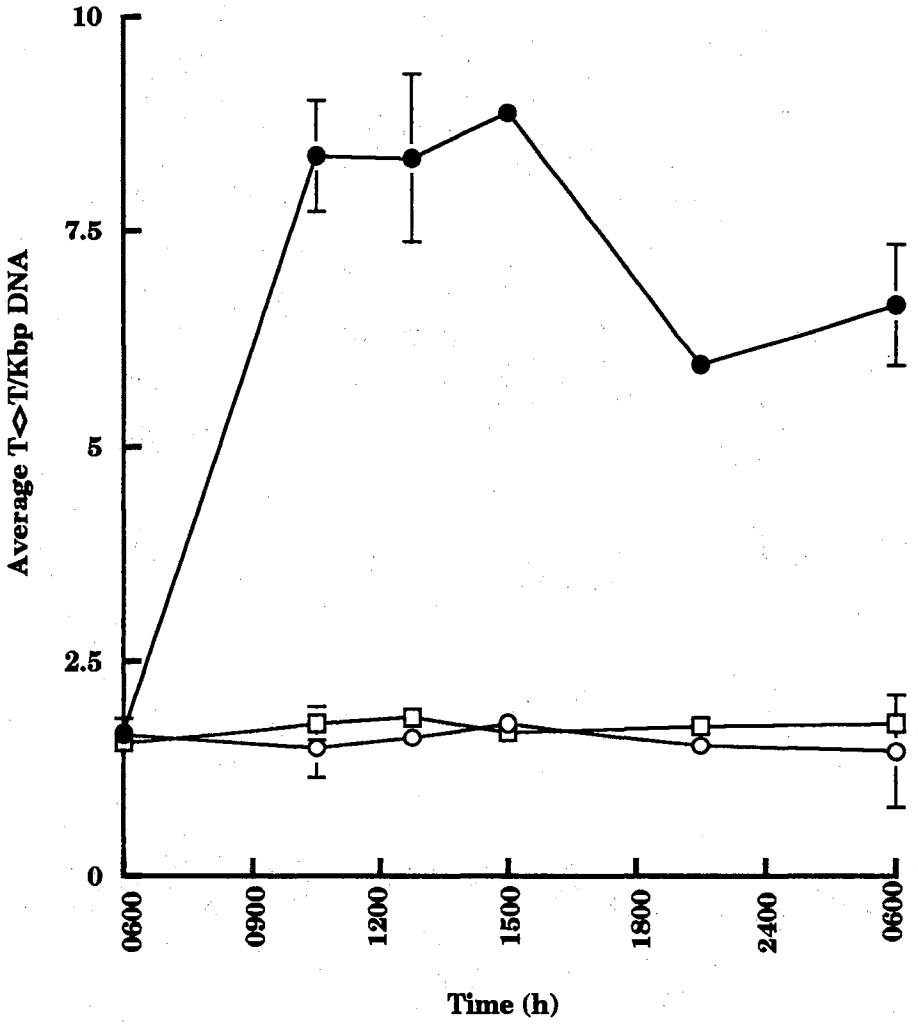

Fig. 18. Accumulation of cyclobutane dimers in *V. natriegens* in *in situ*-mimicking experiments conducted in 1994. Samples for DNA extraction were taken every 4 h over 24 h from solar UV-R-exposed microcosms containing *V. natriegens* cultures. Treatments of microcosms were as follows: unexposed (open circles), exposed to full sunlight (closed circles), and exposed to UV-R-filtered sunlight using an acrylic screen (open squares). Error bars represent the range of duplicate samples taken at each timepoint.

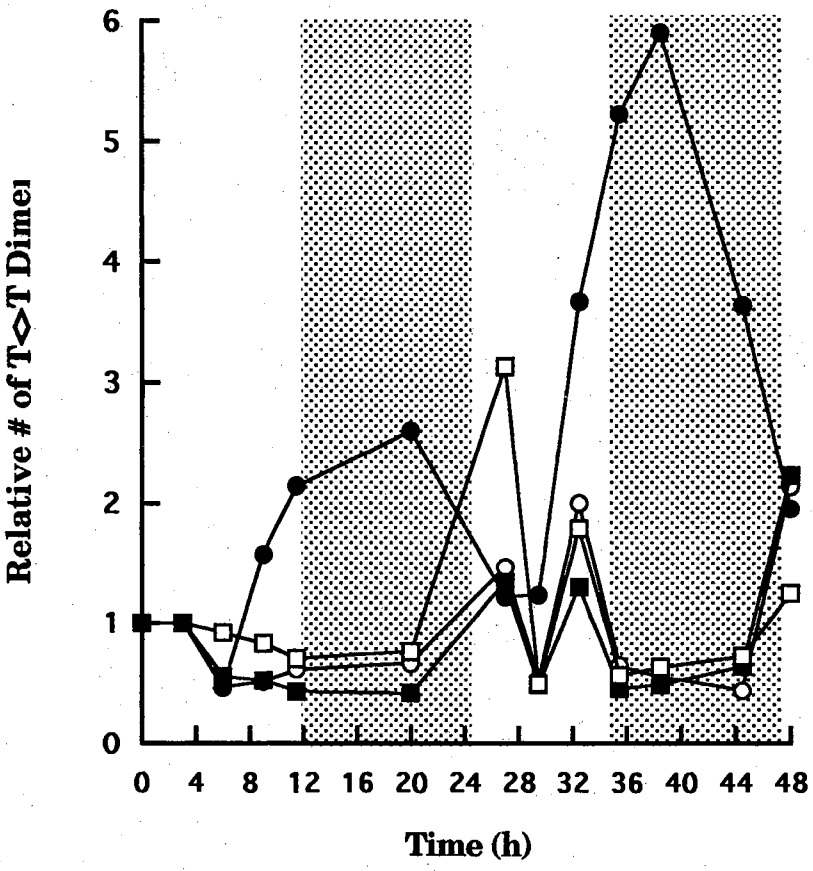

Fig. 19. Accumulation of cyclobutane dimers in *V. natriegens* in *in situ*-mimicking experiments conducted in 1995. Samples for DNA extraction were taken periodically for 48 h from solar UV-R-exposed microcosms containing *V. natriegens* cultures. Microcosms underwent the following treatments: unexposed (open circles), full sunlight (closed circles), UV-B-filtered using a mylar screen (open squares), and UV-R-filtered using an acrylic screen (closed squares). The relative number of T<>T dimers for one experiment conducted on a sunny day in the Gulf of Mexico is represented. For each sample, the number of T<>T dimers is normalized to the number of dimers at the beginning of the experiment. The shaded areas represent the evening (dark) period of recovery.

tion of T<>T was observed in microcosms receiving full UV-R. Two seperate experiments were conducted. For the latter experiment, increment weather may have affected results. Therefore, data from the experiment conducted during a typical sunny day in the Gulf of Mexico is presented in Fig. 19. Dimers samples in 1996 were unavailable.

Technical development. The experiments conducted in microcosms aboard various research vessels proved an excellent method of mimicking a marine environment with a control microorganism. Contamination was kept to a minimum with semi-selective plating, physical barriers and high cell densities. Viability assessment was easily accomplished on board with traditional laboratory serial dilution techniques. For analysis of RecA induction, proteins extracted from cell pellets were more useful for Western analysis than those extracted from filters. However, when studying natural populations, this is not feasible as bacterial densities are not sufficient to produce a pellet with a reasonable volume of filtered seawater. Utilizing 142 mm filter discs and filtering large quantities of seawater (60-L) provides enough material and has been successful.

SDS-PAGE gels provided a clear representation of RecA induction. The slot-blot method facilitated processing large numbers of samples in a reasonable amount of time. Densitometry provided an optical density signifying the amount of antigen:antibody coupled binding to the filter. This was normalized to the number of viable cells from which the protein was extracted. Traditional studies using slot-blot analysis incorporate sample dilution and linear regression as an accepted standard method.

Conclusions

Literature on monitoring rates of DNA repair in microbial communities in the environment is scarce. Studies of other responses often infer repair but do not actually test for it. In this study a method for assaying repair by quantifying the amount of an important repair protein, RecA, was developed. It is clear that RecA is induced by UV-R. More specifically, when speaking of solar UV-R, RecA appears to be induced maximally by lethal dosages of UV-A. Additionally, RecA may be induced in a diel fashion. Thymine dimers appear to accumulate and become repaired in a similar pattern (34), but results shown here do not point to a direct relationship of RecA induction and the formation of T<>T dimers. It is clear that RecA induction is related to an increase in lesion(s) which results in loss of viability which may include T<>T dimers. Viability was shown to be as significantly affected by UV-A as total solar radiation. Recovery was observed overnight in microcosms whether or not cultures received photoreactivating light after UV-R exposure. However, cultures receiving the full solar spectrum were killed to $\geq$95%, a significantly higher degree than those receiving only UV-A (Figs. 11, 12, and 14). Furthermore viability was shown to be impaired at 10 m depths in the water column indicating that the combined effects of UV-B and UV-A are impacting bacterioplankton communities within the water column (Table 2). These data demonstrate that bacterioplankton in the environment are already under stress with which they manage to cope when exposed to current levels of UV-A. However, an increase in UV-B may alter this balance leading to serious consequences for the environment.

As the response to solar ultraviolet radiation is an involved process at both the ecological and molecular level, a study of a single representative of the marine bacterioplankton community utilizing molecular techniques allows us to ask questions about effects of UV-R without interference from other activities contributed by higher trophic levels. Ultimately we would like to learn whether increasing UV-R will detrimentally affect marine productivity. Bacterioplankton are essential to marine food webs and have been shown to be impacted by UV-R, but to what extent and how well they cope is still unclear. It is impossible to draw conclusions on the impact of UV-R at all trophic levels. Therefore examining each level separately will help us to understand how each level responds and interacts with others. Different phytoplankton species are shown to be very different in their responses. Is this true for bacterioplankton? Comparing results from this study of a bacterioplankton representative to similar studies of isolates and results obtained from natural communities will answer this question. Do all members of this community respond in the same manner or do various members cope differently? If the former conclusion is correct, a model such as *V. natriegens* can be routinely used to predict how the bacterioplankton community is responding. However, if the latter conclusion is drawn as indicated by results of this study with an isolated organism in comparison to natural communities, how will this affect the marine ecosystem and energy fluxes?

CHAPTER V

IS THE RESPONSE OF RecA TO ULTRAVIOLET RADIATION WAVELENGTH DEPENDENT?

Introduction

Studies to elucidate the many roles of RecA in prokaryotes have been done utilizing chemical mutagens and UV-C (100-280 nm) light (43). This short wavelength, high energy portion of the ultraviolet spectrum results in damages which elicit the response of RecA (43). In the environment, microorganisms are bombarded daily with ultraviolet radiation which does not include these shorter wavelengths (1, 19, 21 22,34, 35). Both UV-A (320-400 nm) and UV-B (280-320 nm) have been shown to significantly stress microorganisms in the marine environment. RecA has been shown to respond to relevant solar wavelengths which are found to penetrate to the surface in the environment (39), but whether RecA responds to damages caused by the shorter UV-B wavelengths or to impairments caused by longer wavelengths has not been shown.

UV-B results in direct DNA lesions similar to those induced by short wavelength UV-C (12, 32, 49, 61). UV-A, on the other hand, is much more complex and not clearly elucidated as yet. Several studies suggest that a cellular chromophore may absorb the UV-A photon and transfer the

energy to DNA resulting in DNA damage (7, 12, 55, 58). Additionally, oxygen appears to play a significant role in UV-A induced damage (12, 30).

RecA is an essential enzyme in several prokaryotic repair processes. In this study we have investigated the response of RecA in the marine isolate, *V. natriegens*, to discrete portions of the solar UV spectrum utilizing monochromatic and polychromatic light. By understanding how RecA responds to the various segments of the solar UV-R spectrum, its usefulness as a biological dosimeter of DNA repair in marine bacterioplankton communities can be assessed.

Results and Discussion

Viability. Initially, a series of traditional dose-response survival experiments were conducted. Cell suspensions of*V. natriegens* were exposed to various doses of polychromatic UV-C, UV-B, and UV-A to determine the organisms' relative sensitivity UV-R. (Fig. 20) illustrates a monotonic dose-dependent response of *V. natriegens* to artificial polychromatic UV-R. In response to UV-C which has been used to study *P. aeruginosa,* a freshwater aquatic and soil microorganism, and *E. coli,* an enteric microorganism, RecA responses, *V. natriegens,* a free-living marine microorganism, behaves much like *P. aeruginosa*. These data illustrate that doses of 0-100 J/m^2 of UV-C, 0-200 J/m^2 of UV-B and 0-80,000 J/m^2 of UV-A are effective ranges for determining the resistance of *V.natriegens* to UV-R. Lower doses of UV-A were demonstrated to be sublethal as literature suggests (Fig. 20 UV-A "low") (12, 54, 55).

In addition to dosages which reduced bacterial viability, environmentally relevant doses of UV-R were determined and used for this study.

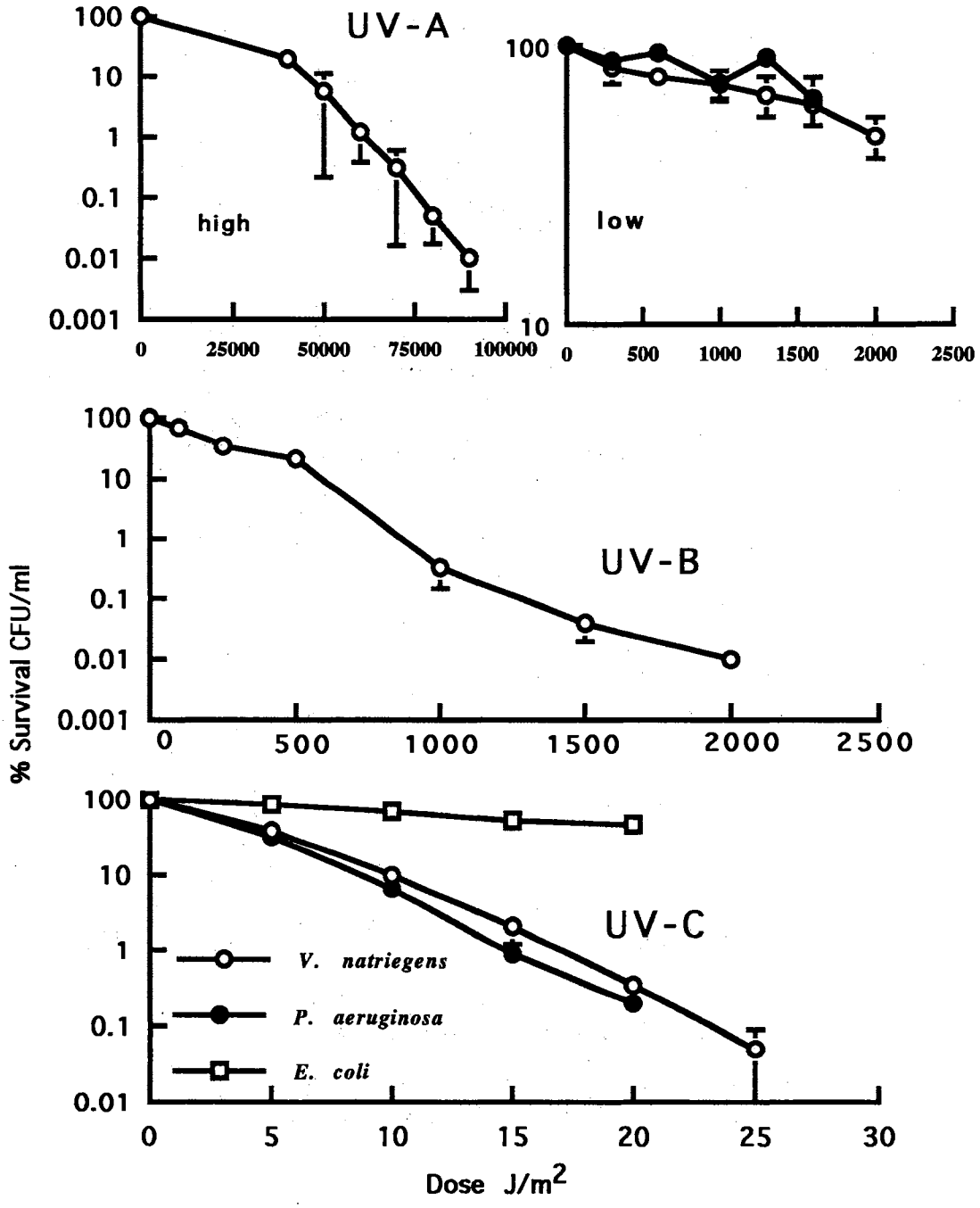

Fig. 20. Survival of *V. natriegens* following exposure to various types of polychromatic UV-R. Information available for other organisms' response is compared. Standard error represents three repetitions of the experiments for each dosage.

Light data gathered from research cruises in the Gulf of Mexico was compiled and averaged. For doses of polychromatic irradiation, amounts received during a full day were compiled for the wavelengths gathered. Doses of UV-A were compiled from daily outputs at 340 nm, 360 nm and 380 nm. Likewise, UV-B doses were compiled at 300 nm, 310 nm and 320 nm. For experiments using monochromatic light, each wavelength was calculated separately. Additionally, information from previous literature was examined and included in consideration of dosages to utilize (6, 16, 37, 72).

Table 3 and table 4 summarize bacterial viability following UV-B or UV-A exposure. Table 5 presents data which suggests that cooperative effects occur when *V. natriegens* is exposed simultaneously to UV-B and UV-A at doses which occur in the environment. *In situ* studies (chapter IV) demonstrate that UV-A significantly impacts bacterial viability, although the full solar spectrum including UV-B does cause a greater loss. These experiments have been designed to demonstrate the dose and spectral response of *V. natriegens* to various segments of the UV-R spectrum. However, we must keep in mind that these studies utilize UV sources with constant flux and fixed spectral output. Neither of these properties is true for sunlight.

Mutagenesis. RecA is involved in several repair processes in the cell including mutagenic DNA repair. In order to assess the DNA-repair potential of *V. natriegens*, Weigle reactivation of UV-C-damaged bacteriophage nt-1 and chromosomal mutagenesis after UV-R exposure were

Treatment	UV Dose J/m^2	Survival rate (%)	Mutation frequency (Rif^r mutants per 10^8 survivors)
Unexposed	0	100 ± 0	2 ± 0.08
UV-C			
	10	1.5 ± 1.55	160.5 ± 82.5
	30	1.73 ± 1.57	100 ± 124.54
UV-B			
	75	10.7 ± 3.2	223 ± 113.7
	125	6 ± 0.71	130 ± 32.2
	360	0.09 ± 0.02	1957 ± 902
	5164	0.00004 ± 0.00003	1×10^7 ± na **
UV-A			
	2000	89 ± 11.1	3.4 ± 5.5
	3600	78 ± 11.5	1 ± 2.2
	20000	10.8 ± 1.2	25.6 ± 15.5
	26800	15 ± 3.2	11.2 ± 6

Table 3. UV-R-induced mutagenesis of the *V. natriegens* chromosome. Cultures of *V. natriegens* were grown to early exponential phase and exposed to various types of polychromatic radiation at various doses. Survival rates and numbers of rifampicin-resistant (Rif^r) mutants were determined by differential plating. Standard error represents at least three different experiments for each dose. **due to the high level of killing in this sample, all samples were found to produce > than 1 million Rif^r mutants per 10^8 survivors.

UV dose to host	Calculation of WRF	WRF
Unexposed	$\frac{1.5 \times 10^{5}{}_{\text{øUV}} / 1.1 \times 10^{8}{}_{\text{ø noUV}}}{1.5 \times 10^{5}{}_{\text{øUV}} / 1.1 \times 10^{8}{}_{\text{ø noUV}}}$	1
UV-C 30 J/m^2	$\frac{1.7 \times 10^{5}{}_{\text{øUV}} / 1.0 \times 10^{7}{}_{\text{ø noUV}}}{1.5 \times 10^{5}{}_{\text{øUV}} / 1.1 \times 10^{8}{}_{\text{ø noUV}}}$	12.5
UV-B 125 J/m^2	$\frac{2.0 \times 10^{5}{}_{\text{øUV}} / 1.0 \times 10^{7}{}_{\text{ø noUV}}}{1.5 \times 10^{5}{}_{\text{øUV}} / 1.1 \times 10^{8}{}_{\text{ø noUV}}}$	14.7
UV-A 3600 J/m^2	$\frac{8.9 \times 10^{4}{}_{\text{øUV}} / 1.0 \times 10^{8}{}_{\text{ø noUV}}}{1.5 \times 10^{5}{}_{\text{øUV}} / 1.1 \times 10^{8}{}_{\text{ø noUV}}}$	0.65

Table 4. Weigle reactivation of UV-C-irradiated bacteriophage nt-1 by *V. natriegens*. Irradiated and unirradiated bacteriophages were used to infect the host bacteria, *V. natriegens*, which had been exposed to doses of polychromatic UV-R. Doses which were shown to induce RecA in *V. natriegens* were selected. The Weigle reactivation factor (WRF) was calculated from the formula in Chapter 3 and is a measure of the inducible DNA repair capacity of the host cell. The differences in the WRF for *V. natriegens* exposed to the different wavelength ranges are significant.

Treatment	Dose (J/m^2)	% Survival	IR RecA (OD/μg/ viable cell	IR CPD/mb T<>T
unexposed	0	100	0.45	1.0
UV-A	22572	50	3.7	0.52
UV-B	2178	20	44.8	28.6
UV-A and UV-B	22572 and 2178	0.002	3.9×10^4	48.5

Table 5. *V. natriegens* response to environmentally-relevant doses of UV-R using artificial polychromatic UV-R sources. Exponential cultures of *V. natriegens* were exposed to the various doses of UV-R. Samples for RecA protein, DNA, and viable counts were taken prior to exposure, directly after, and for two hours following exposure. Doses were selected from light data gathered in the Gulf of Mexico during research cruises and previous literature. IR is the induction ratio of the amount of RecA or dimers in an exposed sample relative to the amount before exposure.

investigated. Previous studies have demonstrated increased repair and mutagenesis after UV-C exposure in *E. coli* , but they are lacking in other species such as *P. aeruginosa* and *Salmonella typhimurium* (43, 45, 69). Although, the dose-response of *V. natriegens* is very similar to *P. aeruginosa*, this organism encodes functional mutagenic repair. In response to polychromatic UV-C and UV-B of the number of Rif^r mutants increases indicating "error-tolerant" or mutagenic repair of the chromosome (Table 3). UV-A does not induce this response. Likewise, UV-damaged phage particles regained significant infectivity in *V. natriegens* which had been exposed to UV-C or UV-B but not UV-A (Table 4). Shorter, high-energy wavelengths < 320 nm appear to be responsible for this affect (Table 5 and Table 6). However, 380 nm exposure resulted in increased Weigle reactivation (Table 6). This wavelength at high doses may result in lesions similar to those caused by shorter wavelengths although the primary chromophore may be different.

RecA Induction. RecA induction was shown to be dose-dependent in response to UV-B (Fig. 21). Low to moderate induction was observed after exposure to high dosages of UV-A (Fig. 21). Likewise when exposed to environmentally relevant doses of each, UV-B induced RecA to a greater extent (Table 5). However, when the two were combined, the result was significantly greater than a simple additive effect. This implies that cooperative or synergistic damages occur when bacteria are exposed to polychromatic UV-R including UV-A and UV-B. In response to monochromatic UV-R, RecA was found to be induced by all wavelengths tested with the exception of 360 nm light. Various doses at this wavelength were

Wavelength (nm)	Dosage (J/m^2)	%Survival (CFU/ml)	WRF	IR RecA (OD/μg/10^6 CFU/ml)	IR CPD/mb T<>T	IR CPD/mb CT DNA
254	1.0	39	140	19.1	1.03	2.75
320	460	28	1.00	8.40	2.20	2.83
360	1000	76	12.1	1.30	0.79	2.50
380	1200	32	2.40	12.0	0.32	2.67

Table 6. *V. natriegens* response after exposure to monchromatic UV-R. Monochoromatic light was generated using an Alexandrite laser. Doses were determined by estimating the dose of each wavelength observed during a full day in the Gulf of Mexico. For the 254 nm wavelength which is not received in Earth's surface environment, a dose observed to induce RecA with polychromatic light was used. WRF is the Weigle reactivation factor utilizing *V. natriegens* bacteriophage nt-1. IR is the induction ratio of samples taken before and after UV-R exposure. Calf thymus DNA (CT DNA) was also included as a cell-free control for T<>T dimer estimates as generated by the Alexandrite laser.

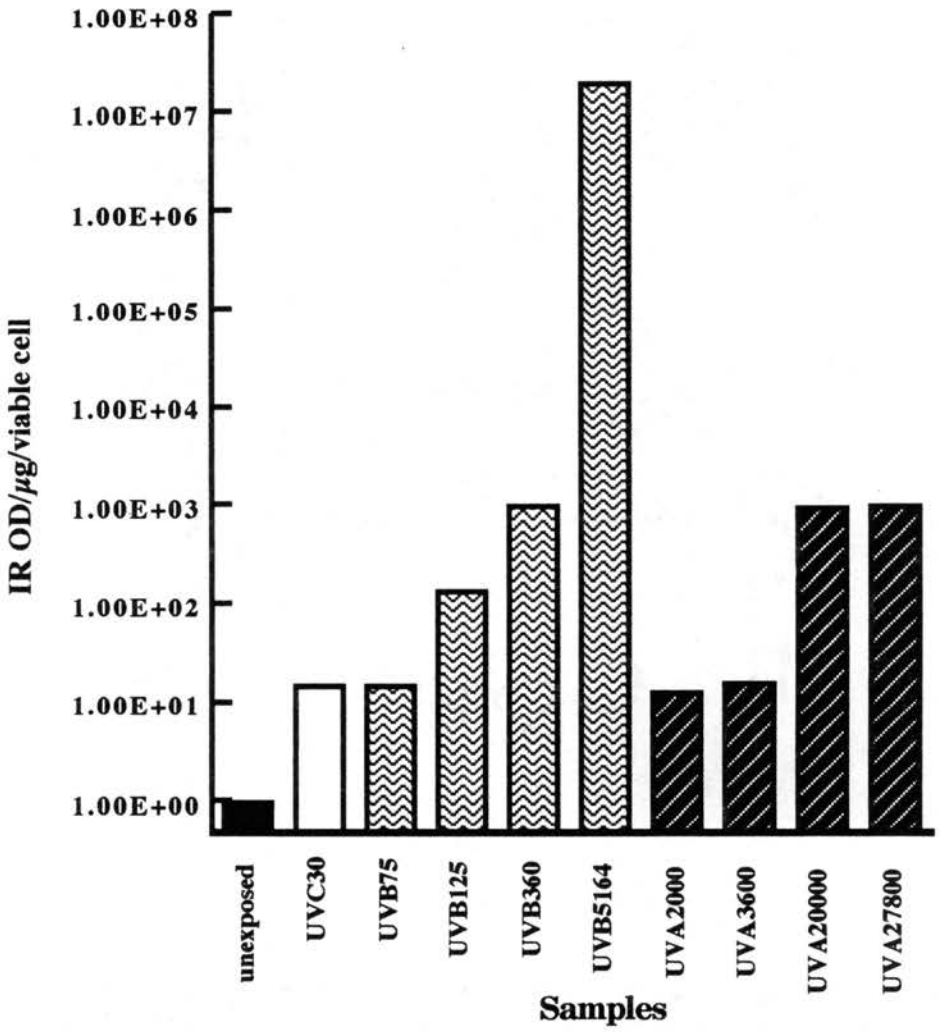

Fig. 21. RecA induction in *V. natriegens* viable cells exposed to polychromatic UV irradiation. Values represent the maximum relative induction of RecA (OD per μg of total protein per viable cell) observed within 4 h of sampling after exposure. Maximum amounts of RecA induction were not necessarily observed at the same time for each dose.

tested with no apparent differences in RecA's response (data not shown). Bacterial survival was notably higher at this wavelength as well. The polychromatic UV-A light sources used for this study also have a peak output at 360 nm. These observations and results together indicate that 360 nm light may specifically activate a photodependent repair mechanism, or photolyase, which is simultaneously repairing any UV-R-induced damage. This may explain why *V. natriegens* viability loss, RecA induction and dimer formation after exposure to monochromatic UV-A at 360 nm or polychromatic UV-A are not observed at levels equal to those observed *in situ* (Chapter 4). RecA induction and Weigle reactivation observed in cells exposed to 380 nm light was higher than those exposed to 360 nm light which further corroborates this hypothesis that 360 nm light may activate a repair mechanism which does not invovle RecA.

DNA photoproducts. Calf thymus DNA was included as a cell-free control in experiments utilizing monochromatic light to rule identify any differences related to whole cell impediments (9, 60, 68). Detectable levels of T<>T dimers were not observed in laser-exposed samples. This is likely an intrinsic factor of the experiment which I have been unable to pinpoint. However, significant dimer formation was observed in cultures exposed to environmentally relevant doses of UV-B and UV-A and UV-B. As viability vastly decreased in cultures exposed to UV-A and UV-B, speculation may suggest the resulting increase in RecA is merely mathematical. Yet, the high number of dimers also formed indicates that UV-A and UV-B may interact to cause cellular damage.

Conclusions

Bacterial viability is significantly affected by both UV-A and UV-B wavelengths. RecA is induced by both wavetypes as well, indicating that this proteinis dynamic in its repair functions. Responding to the various diverse lesions caused by this enzyme does not indicate a wavelength dependent response. However, in this study RecA induction to UV-A-induced damage was not as apparent as *in situ* studies have suggested (Chapter 4). Induction was observed at 380 nm, which may indicate that a specific photodependent repair mechanism or enzyme is activated by 360 nm light produced both monochromatically and polychromatically in this study. This would reduce the need for other repair mechanisms controlled by RecA. When exposed concurrently to UV-A and UV-B, this repair mechanism may be saturated resulting in the loss of viability, dimer formation and RecA production observed.

As global concern over increasing UV-R mounts, the demand for techniques to monitor UV-impact is high. Utilizing fixed sources of UV-R, we have clearly demonstrated that RecA is important in the repair of UV-R-induced damage from 254 nm through 400 nm. Comparing the information gathered here on molecular responses to information obtained *in situ*, RecA serves as a promising candidate for a repair-indicator of UV-R-induced DNA damage in terrestrial and marine bacterial communities.

CHAPTER VI

RecA INDUCTION IN MARINE BACTERIOPLANKTON COMMUNITIES OF ANTARCTICA

Introduction

Most concern over ozone depletion is the reaction to information gathered in the austral spring of Antarctica (14, 71, 73). During October and early November ozone levels drop as much as 60% over this region, often called a "hole", although this is somewhat of a misnomer for what is actually a thinning of this layer in our stratosphere (73). Ozone depletion results in decreased absorption of ultraviolet radiation (UV-R) by the stratosphere and increased UV-R penetration to the earth's surface (14, 16). Up to a 20% increase in biologically effective UV-R is observed in October compared to March in Antarctica (72). Generally, total ozone is depleted in October, but there are large day to day fluctuations, believed to be primarily the result of the polar vortex. Less fluctuations occur after summer solstice (72). As mentioned in Chapter 2, the entire ozone turnover during this crucial time is temperature dependent.

Several studies have been conducted to investigate the impact of increased UV-B on phytoplankton (5, 15, 23, 24, 25, 42, 67, 87). Interestingly, results show that UV-A causes photosynthetic rates to decrease more than UV-B (25). As bacteria are highly diversified and simpler in structure than

phytoplankton, the fate of the overall bacterioplankton community cannot be predicted by results of phytoplankton or single-bacterial-isolate studies. The entire community must be examined as well as several individual representatives.

Results from previous studies in the Gulf of Mexico have shown that marine bacterial productivity, growth rates and accumulation of DNA damage are all significantly affected by solar UV-R (Chapter 4, 1, 8, 34, 35). RecA has been shown to respond to solar UV-R both in the laboratory (Chapter 5) and in a marine isolate (Chapter 4). In this study, natural marine bacterial communities and an Antarctic bacterial isolate have been studied for their DNA-repair response by looking for enhanced RecA expression after exposure to solar UV-R. These experiments further assess the usefulness of using RecA as a monitor of DNA repair. Additionally, the DNA-repair potential of the dynamic, but UV-R-stressed Antarctic marine bacterioplankton community is investigated.

Results and Discussion

Induction of RecA in natural bacterioplankton assemblages. Studies were conducted in October and November of 1995 and 1996 aboard the RV POLAR DUKE in the Gerlache Straits, Antarctica 64 10 °S 61 50°W. Figures 22 and 23 illustrate the induction of RecA at detectable levels in natural bacterioplankton populations receiving ambient sunlight. Surface samples were collected every 2 hours for 24 h for each experiment. The results of the diel experiments performed on different dates were averaged together in order to determine the typical response. Results of diel experiments conducted in 1995 and 1996 were very similar. RecA production peaked

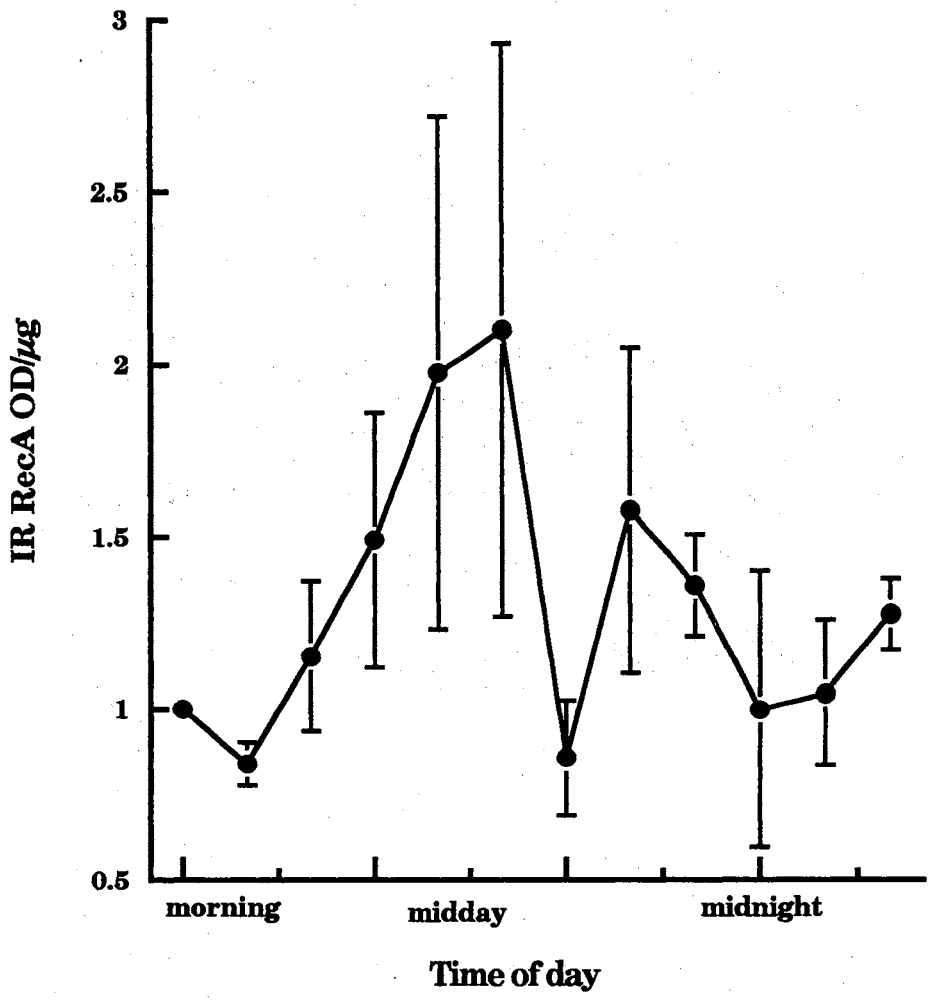

Fig. 22. RecA induction over 24 h in natural marine bacterioplankton in 1995. Diel experiments were averaged together to estimate overall RecA response to solar UV-R in natural marine bacterioplankton populations. Surface samples were collected every 2 h for 24 h for each experiment. The induction ratio (IR) represents the amount of RecA (OD/μg) at each timepoint relative to the amount in the first sample.

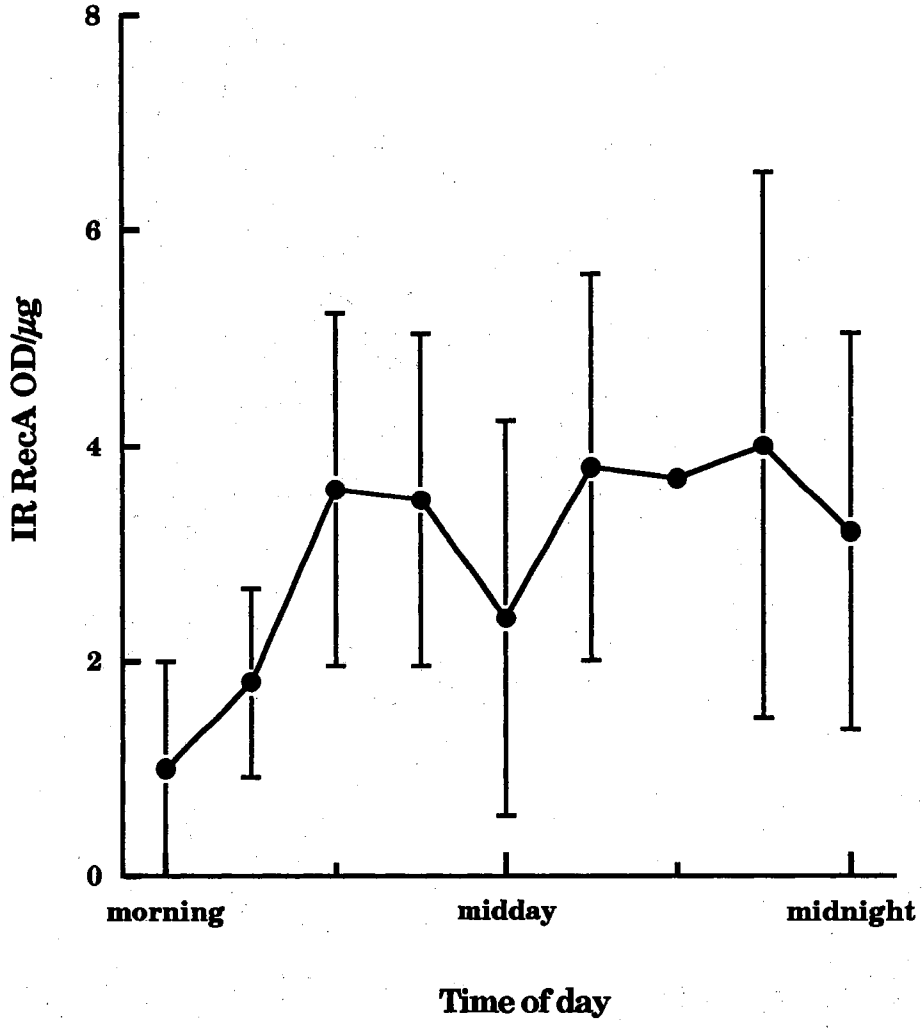

Fig. 23. RecA induction over 24 h in natural marine bacterioplankton in 1996. Diel experiments were averaged together to estimate overall RecA response to solar UV-R in natural marine bacterioplankton populations. Surface samples were collected every 2 h for 24 h for each experiment. The induction ratios (IR) represents the amount of RecA (OD/μg) at each timepoint relative to the amount in the first sample. These experiments were conducted on Oct. 4, 8, 13, 19, 22, 1996.

during the afternoon with a subsequent late afternoon drop. Levels increased again overnight before returning to background levels by morning. The late afternoon drop in RecA is most likely the interplay of photodependent repair mechanisms. As levels of UV-B are attenuated in late afternoon creating higher ratios of UV-A to UV-B, the rate of DNA damage decreases while simultaneously light-activated enzymes function to repair existing lesions. However, as the sun sets, these enzymes are no longer active. The cell signals other repair mechanisms to take up the slack. Therefore, the demand for RecA once again increases.

Response of an Antarctic marine bacterial isolate to solar UV-R. As government regulations disallow the introduction and use of laboratory bacterial strains in Antarctica, three bacterial strains were isolated from seawater. These gram-negative aerobes were further characterized by PCR and sequence analysis utilizing a *recA* probe (L. van Waasbergen, personal communication). Computer analysis of sequences and characterization with BIOLOG (BIOLOG, Inc., Hayward, CA)indicated that these isolates belong to the purple bacteria of the gamma subdivision. Examples of organisms within this subdivision are *Vibrio, Hemophilus, Proteus* and *Pseudomonas*. As complete identification was unnecessary for this study, further characterization was not done. Cross-reactivity of the *E. coli* anti-RecA used for protein analysis is demonstrated in Figure 24.

Two types of experiments were conducted with the Antarctic isolate selected (RM 11001, Table 1) to assess effects dependent on fluence of radiation. The first was to investigate the production of RecA and loss of viability over a 24 h period. The second was to compare loss of viability after

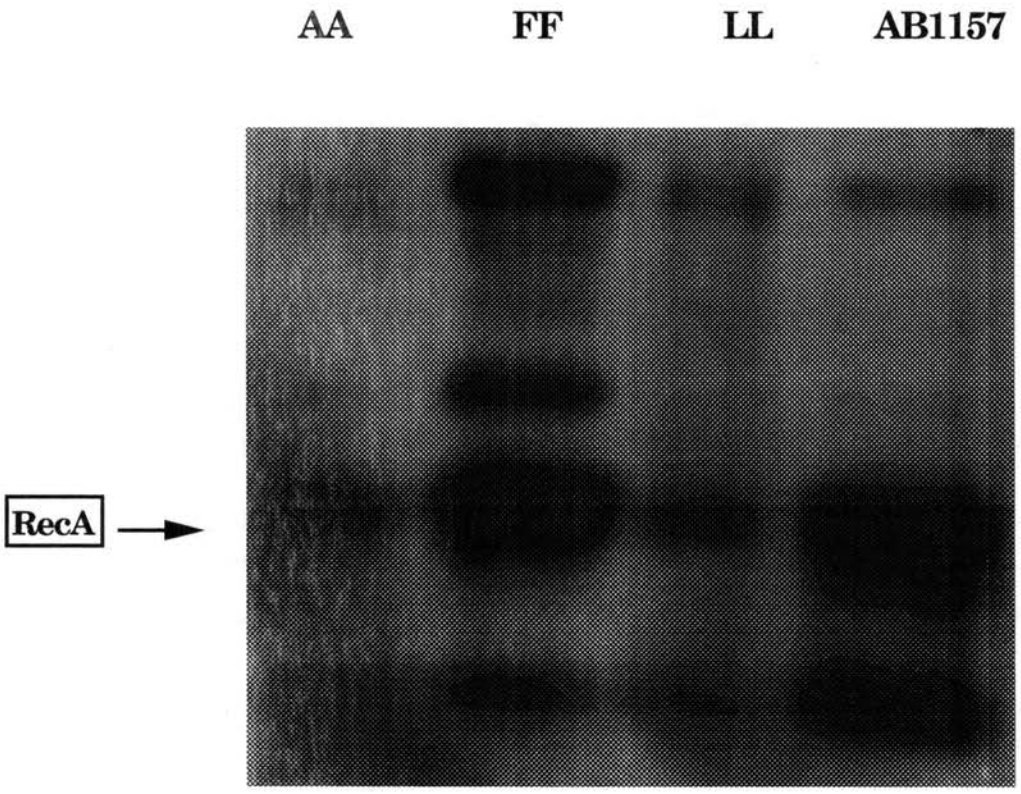

Figure 24. Autoradiograph of Western blot analysis testing *E. coli* anti-RecA antisera against total protein extract of three Antarctic bacterial isolates, RM 11001, RM 11002, and RM 11003. AB1157 was included in the right lane as a positive control.

exposure to sunlight for 2 h followed by treatment with UV-R-filtered sunlight, UV-B-filtered sunlight, full sunlight or darkness for 6 h. Following treatment recovery of cultures was monitored for 48 h.

Previously, RecA induction has been studied in V. *natriegens* in the Gulf of Mexico (Chapter 4). UV-A alone as well as full sunlight (UV-A and UV-B) induced RecA to similar levels in a 24 h pattern. Helbing et al. (21) also demonstrated that bacterial isolates of *Acinetobacter* and *Bacillus* showed increased resistance to UV-A and UV-B if their SOS system was pre-induced by a 1 h exposure to nalidixic acid before exposure to solar UV-R. As RecA is the central mediator of the SOS system (45), these results indicate that a functional RecA does enhance bacterial resistance or DNA repair when exposed to solar UV-R. Figure 25 demonstrates RecA induction in RM 11001 in response to solar UV-R. Significant induction was detected in response to full sunlight. However, only moderate levels of induction are seen in cultures exposed only to UV-A. Additionally, RecA levels did not show the same pattern of induction as *V. natriegens* and natural populations displayed. This organisms' viability was minimally affected by UV-A as well. Taken together, this information illustrates that various members of the bacterioplankton community respond differently to UV-R as has been observed among phytoplankton populations (15, 42, 66, 67, 87). RM 11001 receives higher incident doses of UV-R from time to time and may have adapted (i) efficient photodependent repair mechanisms or (ii) oxidative protection systems. UV-A induced damage is often attributed to the formation of H_2O_2 and oxygen radicals (30). In addition, tRNAs inactivated or altered by UV-A result in growth delays (12, 55, 58).

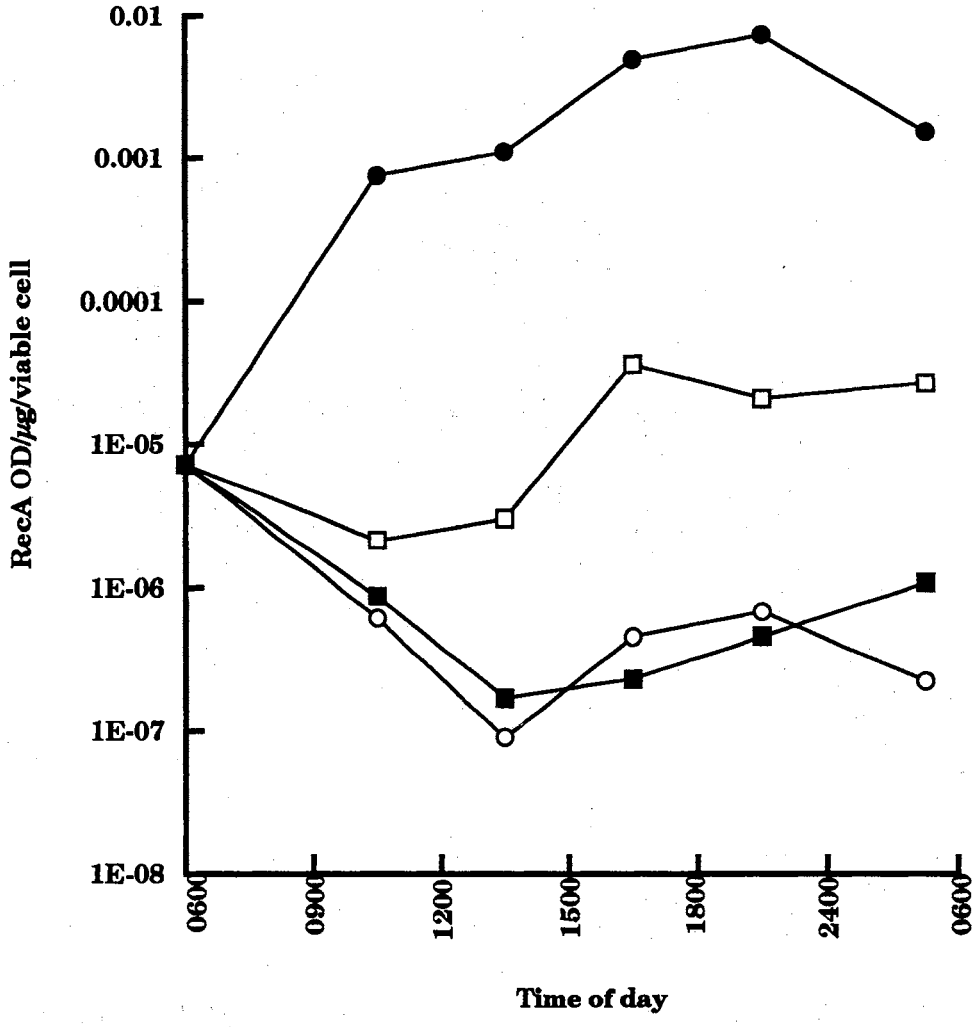

Fig. 25. RecA induction in viable cells of RM11001, a marine Antarctic bacterial isolate, in response to solar UV-R. Treatments included unexposed (open circles), exposure to full sunlight (closed circles), UV-B-filtered sunlight (open squares), and UV-R-filtered sunlight (closed squares). Triplicate cultures were placed under different light treatments and sampled every 4 hours over 24 h for viability and protein extraction for RecA induction analysis.

Figure 26 reveals the isolates' resilience to UV-A. For this experiment, 15 triplicate liquid cell cultures of RM11001 were pre-exposed with 4 h of full sunlight. One triplicate set was destructively sampled for protein extraction and viable counts. The remaining samples were exposed to various light regimes for another 6 h and then transferred to the dark for the remainder of the sampling period. Cells which received further UV-B exposure continued to decline 24 h past treatment. Interestingly, RM11001 cultures which received further UV-A after initial UV-R treatment recovered in the same pattern as cultures which received only PAR or no light at all after initial UV-R exposure. This may indicate two things: (1) RM11001 is more resistant to solar UV-A than previously investigated microorganisms such as *V. natriegens* (Chapter 4); (2) from this experiment, RM11001's higher resistance to UV-A does not appear to be the activity of a photolyase as cultures receiving UV-A, or PAR after initial UV-R exposure did not recover at higher levels than cultures which received no light after initial treatment. On the other hand, one could argue that UV-A or PAR are causing damage at the same rate a putative light-dependent enzyme is repairing damage. Thus, net gain or loss in viability is not observed.

Helbing et al. (21) conducted a similar study with natural marine bacterial assemblages as well as an isolated *Acinetobacter sp.* and a *Bacillus sp.* Viability of natural communities was shown to be more affected than that of the isolates. However, one must keep in mind that the greatest percentage of marine bacteria are unculturable as yet. Studies of bacterial uptake of leucine to demonstrate protein production and uptake of

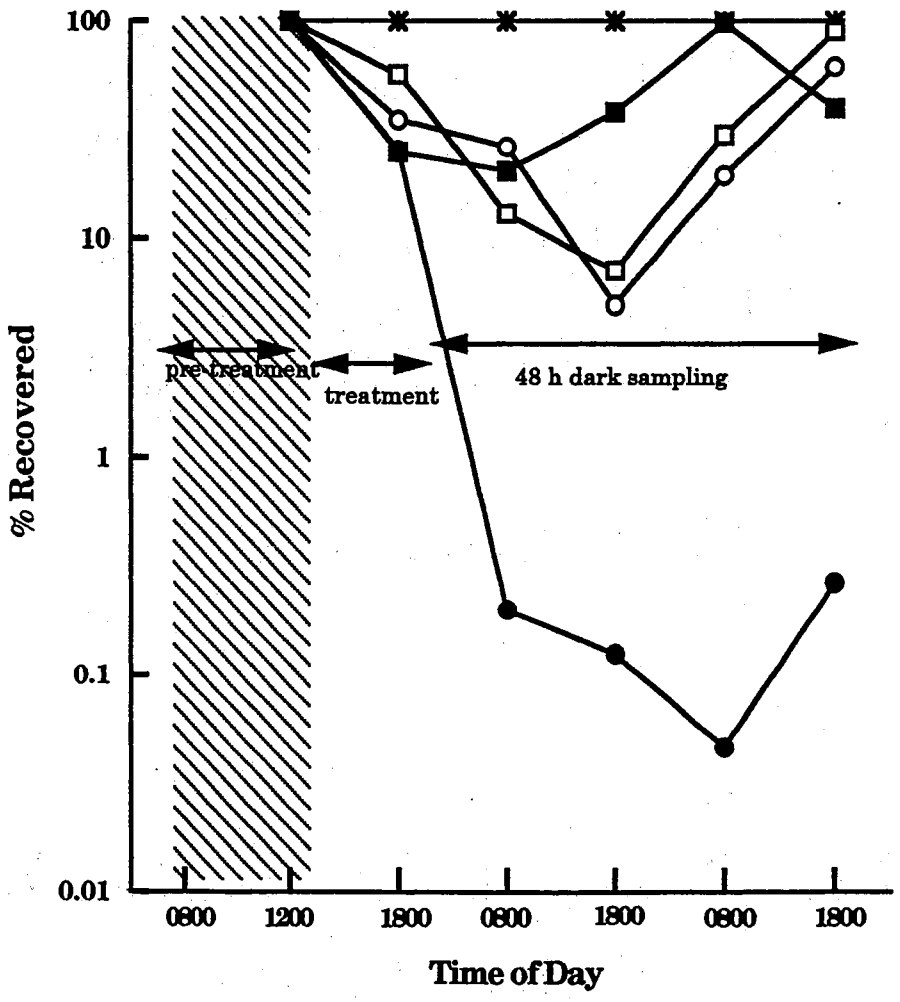

Fig. 26. Recovery of viability of RM11001 after exposure to solar-UV-R under various light conditions. 15 triplicate cultures were pre-exposed to 4 h full sunlight (shaded area) after which 1 triplicate set was destructively sampled and the remaining placed under various light treatments for another 6 h. Treatments included no exposure (open circles),exposure to full sunlight (closed circles), UV-B-filtered sunlight (open squares), and UV-R-filtered sunlight. After treatment all culturess were moved into dark incubation and sampled for viability and protein extraction for later RecA analysis over a period of 48 h. Dark controls were left unexposed for the entire experiment (stars).

thymidine to indicate new DNA synthesis may be better methods for studying productivity and solar UV-R susceptibility in natural marine bacterial communities (1, 8).

Solar radiation information. Light data accumulated from September 27, 1996 to October 26, 1996 are presented in Figure 27 and Table 7. Severe weather patterns and concurrent ozone depletions greatly affected UV-R fluence. In 1996, 5 diel experiments were conducted on October 4-5, October 8-9, October 13-14, October 19-20 and October 22-23. As the dose of UV-R on each of these days was greatly varied, I have averaged these together to estimate a total overall affect to truly reflect conditions encountered by natural populations. Experiments with RM11001 were conducted between October 20-23.

Previous reports have published data demonstrating typical fluences of UV-R at discrete wavelengths during ozone depletion events in Antarctica (6, 16, 37, 72). However, conversion of this information into units easily comparable to those utilized in the laboratory setting when studying molecular responses is time-consuming and tedious. Therefore, I have presented this information in Figure 27, and Table 7 in Joules/m^2 (J/m^2).

Conclusions

The data presented here for the natural bacterial assemblages of bacterioplankton as well as for the isolated bacterial strain, indicate that *recA* induction can be detected following exposure of Antarctic communities to solar UV-R. A consistent 24 h pattern of RecA production was observed in natural populations. Levels peaked in the late afternoon, dipped and rose again during the night before tapering off by morning.

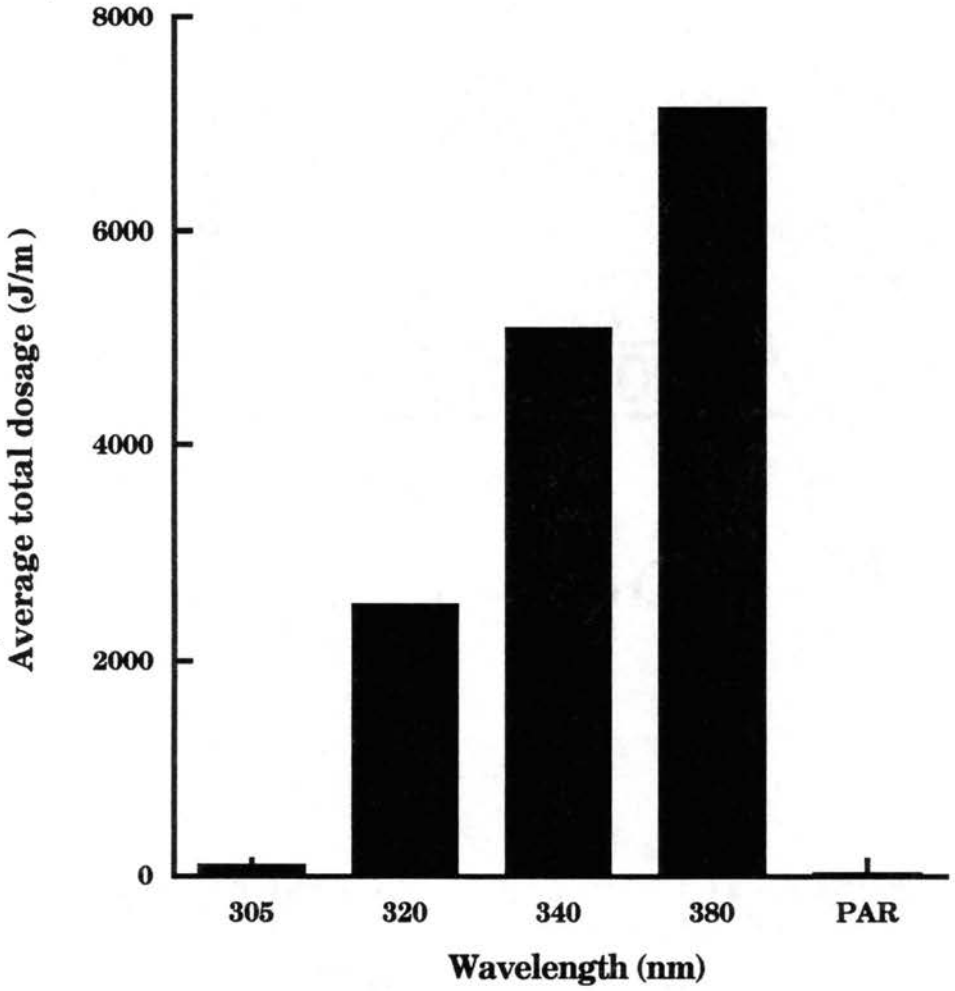

Fig. 27. Average total daily dosage of UV-R at discrete wavelengths. This information was obtained by averaging daily doses from Sept. 27 to Oct. 26 in Antarctica. Further conversion to J/m^2 allows easy comparison to laboratory studies of molecular responses to UV-R.

DATE	Over-all	305 nm		320 nm		340 nm		380 nm		PAR	
9/27	mid	83.4	m	2050	l	4010	m	5700	l	15	m
9/28	low	37.1	l	1040	l	1980	l	2620	l	6.22	l
9/29	low	20	l	1010	l	2090	l	2750	l	6.64	l
9/30	low	28.2	l	1465	l	3222	l	4748	l	14	m
10/1	low	22.7	l	1066	l	2233	l	2923	l	7.11	l
10/12	low	32	l	1760	l	3860	l	5460	l	13.7	m
10/13	mid	50.7	l	2770	m	6100	m	8740	m	21.7	m
10/14	high	63.3	l	3400	h	7350	h	10700	m	27.6	h
10/15	high	134	m	3230	h	6270	m	8950	m	23.1	h
10/16	mid	76.8	m	1780	l	3290	l	4240	l	9.58	m
10/17	high	216	h	3140	h	5530	m	7690	m	19.3	m
10/18	high	222	h	2930	m	5150	m	7050	m	1.72	l
10/20	high	68.4	l	3660	h	7890	h	11000	h	26.5	h
10/21	high	61.0	l	3210	h	6900	m	9680	h	23.5	h
10/24	high	194	m	3580	h	6720	m	9620	h	24.9	h
10/26	high	73.1	m	4050	h	8710	h	12100	h	28.7	h
range		20-222		1010-4050		1980-8710		2620-12100		1.72-28.7	
median		121		2530		5345		7360		15.21	
mean		86.4		2508.8		5081.6		7123.3		16.8	
st.er.		16		251		526		759		2.11	

Table 7. Total fluences of UV-R and PAR obtained daily during austral spring of 1996 presented in J/m^2. Based on ranges obtained for each discrete wavelength (305, 320, 340, 360, 380 nm and PAR) each have been designated as low- (l), mid- (m), or high- (h) range. Likewise overall fluence of all wavelengths combined is characterized for each day.

This signature was similar to that observed for *V. natriegens* in the Gulf of Mexico (Chapter 4).

Although RecA was induced in the Antarctic isolate, its signature differed as RecA levels remained high over 24 h. This suggests residual DNA lesions were as yet undergoing repair throughout the night and suggests a reduced capacity for dark repair. Additionally, *recA* was not induced to the same magnitude in cells exposed to UV-A as those exposed to full sunlight. This observation differs from those made within *V. natriegens*. Likewise, viability was not greatly impacted in RM11001 by UV-A as observed in other microorganisms (25, 36). This species may have adapted protective mechanisms other than dark repair or pigments for UV-A resistance. Undoubtedly, various residents of the marine microbial community have various tolerances and defenses to solar UV-R. Therefore, individual studies of single species cannot be extrapolated to predict future UV-R effects on natural marine assemblages. Comparison of divergent species and their various responses can expand our knowledge of marine communities. Isolates are also useful for studying specific cellular responses such as RecA induction after UV-R stress.

Recently, studies have investigated DNA damage in marine bacterioplankton (34, 35). However, little is known about the DNA-repair capacity of this community which faces daily UV-R challenge. In this study the ability to detect induction of RecA in response to solar UV-R has been demonstrated. By correlating damage estimates with repair assessments, future studies may successfully utilize this correlation as a biologi-

cal dosimeter of total UV-R-induced damage in marine bacterial communities.

CHAPTER VII

CONCLUSION

For centuries scientific research has sought answers to important questions or problems. However, all too often various disciplines remain isolated, unwilling to compromise particular viewpoints on certain topics. Yet, as humanity has come to recognize its influence on the environment as well as its own potential to improve people from various disciplines are beginning to work together to bring about solutions.

An excellent example is the multi-disciplinary effort from around the globe to clean up the Exxon-Valdez oil spill. People with backgrounds in chemistry, oceanography, engineering, biology, microbiology and countless others worked together to rectify a seemingly unsurmountable problem. Cooperative efforts to answer more philosophical questions would also benefit from such teamwork.

In this study, the question "How will ozone depletion and increasing UV-R effect the environment?" was addressed from the viewpoint of a microbiologist. Within my own study, a variety of disciplines have been applied to answer various questions which are my contribution to the "big question". As a microbiologist, I have investigated the responses of marine microorganisms to solar UV-R. I have determined that discrete segments

of the ultraviolet spectrum elicit different responses. UV-A can exclusively impact bacterial viability. UV-B results in greater accumulation of DNA damage. Functioning as a molecular biologist, I examined the function of the RecA in response to UV-R. This protein was shown to be induced by both UV-A and UV-B irradiation. Utilizing fixed spectral sources UV-B elicited a greater response than UV-A. In addition, 360 nm monochromatic light did not induce RecA. This suggests that a repair mechanism which does not require RecA is induced by 360 nm light. In contrast, RecA appeared to be induced by UV-A when the source of UV-R was the sun.

As an ecologist, my task was to learn whether *recA* gene expression is induced in natural settings and to develop techniques to assay this response. Studies conducted in the Gulf of Mexico and the Gerlache Straits, Antarctica utilizing molecular techniques indicated that RecA is induced under natural conditions in a marine isolate and in indigenous microbial communities. Results from this study can be used to estimate DNA damage and repair in marine bacterioplankton communities. These data combined with estimates of productivity, responses of other trophic levels to UV-R and meteorological data will ultimately answer our question of increasing UV-R effects due to reduction in stratospheric ozone.

Although global thinking and interdisciplinary study is at hand, current trends in political correctness often assign scientists to specific niches within their own discipline. One might label me a "molecular microbial ecologist". Niches create bias and squelch expansive scientific thought. Therefore, and only when necessary, I will accept being limited to "microbiologist" . But, truly as a scientist, I believe freedom from restric-

tions allows us to ponder the answers to questions which have yet to be asked.

BIBLIOGRAPHY

1. Aas, P., M.M. Lyons, R. Pledger, D.L. Mitchell, and W.H. Jeffrey. 1996. Inhibition of bacterial activities by solar radiation in nearshore waters and the Gulf of Mexico. Aqua. Microb. Ecol. 11:229-238.

2. Anonymous. 1997. Biotechniques. 22(3):454-456.

3. Azam, F., T. Fenchel, J. Field, J. Gray, L.A. Meyer-Reil, and F. Thingstad. 1983. The ecology of water column microbes in the sea. Mar. Ecol. Prog. Ser. 10:257-263.

4. Bailey, C. A., R. A. Neihof, and P. S. Tabor. 1983. Inhibitory effect of solar radiation on amino acid uptake in Chesapeake Bay bacteria. Appl. Environ. Microbiol. 46:44-49.

5. Bidigare, R. R. 1989. Potential effects of UVB radiation on marine organisms of the southern Ocean:distributions of phytoplankton and krill austral spring. Photochem. Photobiol. 50:469-477.

6. Caldwell, M. M., R. Robberecht, and W. D. Billings. 1980. A steep latitudinal gradient of solar ultraviolet-B radiation in the arctic-alpine life zone. Ecol. 61(3):600-611.

7. Coetzee, W. F., and E. C. Pollard. 1974. Near-UV effects on the induction of prophage. Radiation Research. 57:319-331.

8. Coffin, R. B., D. Velinsky, R. Devereux, W. A. Price, and L. Cifuentes. 1990. Stable carbon isotope analysis of nucleic acids to trace sources of dissolved substrates used estuarine bacteria. Appl. Environ. Microbiol. 56:2012-2020.

9. Coohill, T. P. 1991. Photobiology School: Action spectra again? Photochem. Photobiol. 54:859-870.

10. Coohill, T. P. 1997. UV action spectra for marine phytoplankton. Photochem. Photobiol 65: 259-260.

11. Demidov, V. V., V. N. Potaman, and B. S. Kogan. 1991. Express analysis of DNA photosensitizers. Nuc. Acids. Res. 19(8):1947.

12. Eisenstark, A. 1987. Mutagenic and lethal effects of near-ultraviolet radiation (290-400 nm) on bacteria and bacteriophage. Environ. Molec. Mut. 10:317-337.

13. El-Sayed, S. Z. 1988. Fragile life under the ozone hole. Natural History. October:73-88.

14. Farman, J. C., B. G. Gardiner, and J. D. Shanklin. 1985. Large losses of total ozone in Antartica reveal seasonal CLOx/NOx interactions. Nature. 315:207-210.

15. Forster, R. M., and Luning, K. 1996. Photosynthetic response of *Laminaria digitata* to ultraviolet-A and ultraviolet-B radiation. Scientia marina. 60:65-71.

16. Frederick, J. E., and H. E. Snell. 1988. Ultraviolet radiation levels during the Antarctic spring. Science. 241:438-440.

17. Friedberg, E. C., G.C. Walker, and W. Siede. 1995. DNA repair and mutagenesis. ASM Press, Washington, D.C.

18. Fuhrman, J. A., T.D. Sleeter, C.A. Carlson, and L.M. Proctor. 1989. Dominance of bacterial biomass in the Sargasso Sea and its ecological implications. Mar. Ecol. Prog. Ser. 57:207-217.

19. Gates, F. L. 1930. A study on the bacteriocidal action of ultraviolet light. III. The absorption of of ultraviolet light by bacteria. J. Gen. Physiol. 14:31-42.

20. Geise, A. C. 1976. Living with our sun's ultraviolet rays. Plenum Press, New York.

21. Helbling, E. W., E. R. Marguet, V. E. Villafane, and O. Holm-Hansen. 1995. Bacterioplankton viability in Antarctic waters as affected by solar ultraviolet radiation. Mar. Ecol. Prog. Ser. 126:293-298.

22. Herndl, G. J., G. Miller-Niklas, and J. Frick. 1993. Major role of ultraviolet-B in controlling bacterioplankton growth in the surface layer of the ocean. Nature. 361:71-72.

23. Herrmann, H., D.P. Hader, and F. Ghetti. 1997. Inhibition of photosynthesis by solar radiation in *Dunaliella salina*: relative efficiencies of UV-B, UV-A and PAR. Plant, Cell and Environment. 20:359-365.

24. Holm-Hansen, O. 1997. Short- and long-term effects of UVA and UVB on marine phytoplankton productivity. Photochem. Photobiol. 65(2):266-267.

25. Holm-Hansen, O., E. W. Helbing, and D. Lubin. 1993. Ultraviolet radiation in Antarctica:Inhibition of primary production. Photochem. Photobiol. 58(4):567-570.

26. Hooper, A. B., and K. R. Terry. 1974. Photoinactivation of ammonia oxidation in *Nitrosomonas*. J. Bacteriol. 119:899-906.

27. Horneck, G. 1995. Quantification of the biological effectiveness of environmental UV radiation. J. Photochem. Photobiol. B: Biol. 31:43-49.

28. Horrigan, S. G., A. F. Carlucci, and P. M. Williams. 1981. Light inhibition of nitrification in sea-surface films. J. Mar. Res. 39:557-565.

29. Huffman, R. E. 1992. Atmospheric ultraviolet remote sensing. Academic Press, San Diego.

30. Imlay, J. A., and S. Linn. 1988. DNA damage and oxygen radical toxicity. Science. 240:1302-1309.

31. Jagger, J. 1972. Growth delay and photoprotection induced by near-ultraviolet light, p. 383-401. *In* U. Gallo and L. Santamaria (ed.), Research progress in organic, biological and medicinal chemistry, vol. 3. North-Holland publishing, Amsterdam.

32. Jagger, J. 1985. Solar-UV actions on living cells. Praeger publishers, New York.

33. Jeffrey, W. A., and D.L. Mitchell. 1997. Mechanisms of UV-induced DNA-damage and response in marine microorganisms. Photochem. Photobiol. 65:260-263.

34. Jeffrey, W. H., R.J. Pledger, P. Aas, S. Hager, R.B. Coffin, R. Von Haven, D.L. Mitchell. 1996. Diel and depth profiles of DNA photodamage in bacterioplankton exposed to ambient solar ultraviolet radiation. Mar. Ecol. Prog. Ser. 137:283-291.

35. Jeffrey, W. H., P. A., M.M. Lyons, R.B. Coffin, R.J. Pledger, and D.L. Mitchell. 1996. Ambient solar radiation-induced photodamage in marine bacterioplankton. Photochem. Photobiol. 64(3):419-427.

36. Kaiser, E. and G. J. Herndle. 1997. Rapid recovery of marine bacterioplankton activity after inhibition by UV radiation in coastal waters. Appl. Environ. Microbiol. 63:4026-4031.

37. Karentz, D., and L. H. Lutze. 1990. Evaluation of biologically harmful UV radiation in Antarctic with a biological dosimeter designed for aquatic environments. Limnol. Oceanogr. 35(3):549-561.

38. Karentz, D., F. S. McEuen, M. C. Land, and W. C. Dunlap. 1991. Survey of mycosporine-like compounds in Antarctic marine organisms: potential protection from ultraviolet exposure. Mar. Biol. 108:157-166.

39. Kidambi, S., M. G. Booth, T. A. Kokjohn, and R. V. Miller. 1996. *recA*-dependence of the response of *Pseudomonas aeruginosa* to UVA and UVB irradiation. Microbiol. 142:1033-1040.

40. Klamen, D. L., and R. W. Tuveson. 1982. The effect of membrane fatty acid composition on the near-UV (300-400 nm) sensitivity of *Escherichia coli* K 1060. Photochem.Photobiol. 35:167-173.

41. Malloy, K. D., M.A. Holman, D. Mitchell, H.W. Detrich. 1997. Solar UVB-induced DNA-damage and photoenzymatic DNA repair in Antarctic zooplankton. Proc. Natl. Acad. Sci. 94:1258-1263.

42. Marchant, H. J., A. T. Davidson, and G. J. Kelly. 1991. UVR-protection compounds in the marine algae *Phaeocystis pouchetti* from Antarctica. Mar. Biol. 109:391-395.

43. Miller, R. V. 1992. *recA*, p. 509-517. *In* S. Luria (ed.), Encyclopedia of microbiology. Academic Press, San Diego, CA.

44. Miller, R. V., and T. A. Kokjohn. 1988. Expression of the *recA* gene of *Pseudomonas aeruginosa* PAO is inducible by DNA-damaging agents. J. Bacteriol. 170:2385-2387.

45. Miller, R. V., and T. A. Kokjohn. 1990. General microbiology of *recA*:: Environmental and evolutionary significance. Ann. Rev. Microbiol. 44:365-394.

46. Mitchell, D. L., D. E. Brash, and R. Nairn. 1990. Rapid repair kinetics of pyrimidine (6-4) primidone photoproducts in human cells are due to excision rather than conformational change. Nuc. Acids. Res. 18:963-971.

47. Mitchell, D. L., and J. M. Clarkson. 1981. The development of a radioimmunoassay for the detection of photoproducts in mammalian cell DNA. Biochimica. et Biophysica. Acta. 655:54-60.

48. Mitchell, D. L., J. Hen, and J. E. Cleaver. 1992. Sequence specificity of cyclobutane dimers in DNA treated with solar (UVB) radiation. Nuc. Acids. Res. 20(2):225-229.

49. Mitchell, D. L., and R. S. Nairn. 1989. The biology of the (6-4) photoproduct. Photochem. Photobiol. 49(6):805-819.

50. Muller-Niklas, G., A. Heissenberger, S. Puskaric, and G. J. Herndle. 1995. Ultraviolet-B radiation and bacterial metabolism in coastal waters. Aquat. Microb. Ecol. 9:111-116.

51. Murphy, T. M. 1975. Effects of UV radiation on nucleic acids, p. 3-21 - 3-44. *In* D. S. Nachtwey, M. M. Caldwell, and R. H. Biggs (ed.), Impacts on climate change in the Biosphere, Part 1: Ultraviolet radiation effects (CIAP monog. 5), vol. 1. U.S. Department of Transportation, Springfield, VA.

52. Nicholson, W. L. 1995. Photoreactivation in the genus *Bacillus*. Current Microbiology. 31:361-364.

53. Nunez, M., B. Forgan, and C. Roy. 1994. Estimating ultraviolet radiation at the earth's surface. Int. J. Biometerol. 38:5-17.

54. Peak, M. J., and J. G. Peak. 1982. Lethality in repair-proficient *Escherichia coli* after 365 nm ultraviolet irradiation is dependent on fluence rate. Photochem. Photobiol. 36:103-105.

55. Peak, M. J., and J. G. Peak. 1986. Molecular photobiology of UVA, p. 42-53. *In* F. Urbach and R. W. Gange (ed.), The biological effects of UVA radiation. Praeger Publishers, New York, NY.

56. Peak, M. J., and J. G. Peak. 1989. Solar-ultraviolet-induced damage to DNA. Photodermatol. 6:1-15.

57. Peak, M. J., and J. G. Peak. 1983. Use of action spectra for identifying molecular target mechanisms of action of solar ultraviolet light. Physiol. Plant. 58:367-372.

58. Peters, J. 1977. *In vivo* photoinactivation of *Escherichia coli* ribonucleotide reductase by near-ultraviolet light. Nature. 267:546-548.

59. Porter, K. G., and Y.S. Feig. 1980. The use of DAPI for identifying and counting aquatic microflora. Limnol. Oceanog. 25(5):943-948.

60. Regan, J. D., W. L. Carrier, H. Gucinski, B. L. Olla, H. Yoshida, R. K. Fujimura, and R. I. Wicklund. 1992. DNA as a solar dosimeter in the ocean. Photochem. Photobiol. 56:35-42.

61. Rosenberg, M., and H. Echols. 1991. Differential recognition of ultraviolet lesions by RecA protein. J. Biol. Chem. 265:20641-20645.

62. Rosenstein, B. S., and D. L. Mitchell. 1987. Action spectra for the induction of pyrimidine (6-4) pyrimidone photoproducts cyclobutane pyrimidine dimers in normal human skin fibroblasts. Photochem. Photobiol. 45(6):775-780.

63. Rowland, F. S. 1991. Stratospheric ozone in the 21st century: The chlorofluorocarbon problem. Environ. Sci. Technol. 25:622-628.

64. Rundel, R. D. 1983. Action spectra and estimation of biologically effective UV radiation. Physiol. Plant. 58:360-366.

65. Saunders, S. 1990. Isolation of chromosomal DNA from gram-negative bacteria. Focus. 11:47.

66. Scherer, S., T. Chen, and P. Boger. 1988. A new UVA/B protecting pigment in the terrestrial cyanobacteria *Nostoc commune*. Pl. Physiol. 88:1055-1057.

67. Schick, J. M., M. P. Lesser, W. C. Dunlap, W. R. Stochaj, B. E. Chalker, and J. W. Won. 1995. Depth-dependent responses to solar UVR and oxidative stress in zooanthelate coral *Aoropora micropthalma*. Mar. Biol. 122:41-51.

68. Setlow, R. B. 1974. The wavelengths in sunlight effective in producing skin cancer: a theoretical analysis. Proc. Natl. Acad. Sci. 71:3363-3366.

69. Simonson, S. C., T.A. Kokjohn, and R.V. Miller. 1990. Inducible UV repair potential of *Pseudomonas aeruginosa* PAO. J. Gen. Microbiol. 136:1241-1249.

70. Smith, R. C. 1989. Ozone, middle UV radiation and the aquatic environment. Photochem. Photobiol. 50:459-468.

71. Solomon, S., R. R. Garcia, F. S. Rowland, and D. J. Wuebbles. 1986. On the depletion of the Antarctic ozone. Nature. 321:755-758.

72. Stamnes, K., J. Slusser, M. Bowen, C. Booth, and T. Lucas. 1990. Biologically effective ultraviolet radiation, total ozone abundance, and cloud optical depth at McMurdo station, Antarctica September 15, 1988 though April 15, 1989. Geophy. Res. Lett. 17:2181-2184.

73. Stolarski, R. S. 1988. The Antarctic ozone hole. Scient. Amer. 258:30-36.

74. Sutherland, J. C., and K. P. Griffin. 1984. p-aminobenzoic acid can sensitize the formation of pyrimidine dimers in DNA: direct chemical evidence. Photochem. Photobiol. 40:391-394.

75. Swenson, P. A., and R. B. Setlow. 1970. Inhibition of the induced formation of tryptophanase in *Escherichia coli* by near-ultraviolet radiation. J. Bacteriol. 102:815-819.

76. Tomalsky, M. E., A.E. Gammie, and J.H. Crosa. 1992. Characterization of the *recA* gene of *Vibrio anguillarium*. Gene. 110:41-48.

77. Turley, C. M. 1993. Direct estimates of bacterial numbers in seawater samples without incurring cell loss due to sample storage, p. 143-147. *In* P. F. Kemp (ed.), Handbook of methods in aquatic microbial ecology. Lewis publishers, Boca Raton.

78. Tuveson, R. W., and M. E. March. 1980. Photodynamic and sunlight inactivation of *Escherichia coli* strains differing in sensitivity to near and far UV. Photochem. Photobiol. 31:287-289.

79. Tyrell, R. M. 1995. Biological dosimetry and action spectra. J. Photochem. Photobiol. B: Biol. 31:38-41.

80. Urbach, F. 1989. The biological effects of increased UV radiation: an update. Photochem. Photobiol. 50:439-441.

81. Vaughan, D. R. A. 1995. Remote Sensing Bulletin. Intl. J. of Remote Sensing. 16:763-764.

82. Walker, G. C. 1984. Mutagenesis and inducible responses to deoxyribonucleic acid damage in *Escherichia coli*. Microbiol. Rev. 48:60-93.

83. Webb, A. R. 1995. Measuring UV radiation: a discussion of dosimeter properties, uses and limitations. Photochem. Photobiol. 31:9-13.

84. Weigle, J. J. 1953. Induction of mutation in a bacterial virus. Proc. Natl. Acad. Sci. 39:628-636.

85. Weinbauer, M. G., Wilhelm, S.W., Suttle, C.A., and D. R. Garza. 1997. Photoreactivation compensates for UV damage and restores infectivity to natural marine virus communities. Appl. Environ. Microbiol. 63:2200-2205.

86. Zachary, A. 1978. An ecological study of bacteriophages of *Vibrio natriegens*. Can. J. Microbiol. 24:321-324.

87. Zagarese, H. E., M. Feldman, and C.E. Williamson. 1997. UV-B-induced damage and photoreactivation in three species of *Boeckella* (Copepoda, Calanoida). J. Plankton Res. 19:357-367.

88. Zepp, R. G., T.V. Callaghan and D.J. Erickson. 1995. Effects of increased solar ultraviolet radiation on biogeochemical cycles. Ambio. 24:174-180.

89. Zerefos, C. S., C. Meleti, A.F. Bais, and A. Lambros. 1995. The recent UVB variability over southeastern Europe. J. Photochem. Photobiol. B: Biology. 31:15-19.

VITA

Melissa Booth

Candidate for the Degree of

Doctor of Philosophy

Thesis: SOLAR ULTRAVIOLET RADIATION AND THE ROLE OF RECA IN MARINE BACTERIA

Major Field: Microbiology, Cell, & Molecular Biology

Education: Graduated from the Oklahoma State University with a Bachelor of Science degree in Biology, May 1991. Completed the requirements for the Doctor of Philosophy degree with a major in Microbiology at Oklahoma State University in December 1997.

Professional Memberships: American Society for Microbiology, Sigma Xi, Oklahoma Academy of Science, American Society of Limnology and Oceanography